Systems & Control Letters 175 (2023) 105513

Contents lists available at ScienceDirect

Systems & Control Letters

journal homepage: www.elsevier.com/locate/sysconle

Adaptive quantized control of uncertain nonlinear rigid body systems☆

Siri Marte Schlanbusch, Jing Zhou *

Department of Engineering Sciences, University of Agder, 4879 Grimstad, Norway

ARTICLE INFO

Article history:
Received 24 March 2022
Received in revised form 9 January 2023
Accepted 20 March 2023
Available online xxxx

Keywords:
Adaptive control
Quantization
Backstepping
Rigid body

ABSTRACT

This paper investigates the attitude tracking control problem for uncertain nonlinear rigid body systems, where both inputs and states are quantized. It is common in networked control systems that sensor and control signals are quantized before they are transmitted via a communication network. An adaptive backstepping control algorithm is developed for a class of uncertain multiple-input multiple-output (MIMO) systems where a class of sector bounded quantizers is considered. It is shown that all the closed-loop signals are ensured uniformly bounded and tracking is achieved. Further, the tracking errors are shown to converge towards a compact set containing the origin and the set can be made small by the choice of the quantization parameters and the control parameters. For illustration of the proposed control scheme, experiments were conducted on a 2 degrees-of-freedom (DOF) helicopter system.

1. Introduction

Quantized control has gained increasing interest during the past decades due to the use of information technology in the development of modern engineering applications, such as digital control systems and networked control systems. A quantizer maps a continuous signal into a set of discrete values and introduces nonlinear errors that need to be handled. Quantization is not only inevitable owing to the widespread use of digital processors, but also useful due to the advantage of reducing occupation rate of transmission bandwidth in the communication of signals, see e.g. [1].

The quantized feedback stabilization problem for linear systems where the dynamics are precisely known, has been considered in [1–4]. In [1], it was shown that a logarithmic quantizer is the coarsest one to stabilize a single input linear system, where the number of control values is finite. This work was extended in [3] to consider stabilization of multiple input linear systems.

Stabilization of nonlinear systems in presence of quantization has been investigated in [5–9]. The main results in [1] was further extended to single input nonlinear systems in [5], and for nonlinear uncertain systems in [6–8], where two different adaptive approaches were used in [6,7], while a robust approach was considered in [8]. If there are uncertainties to the system, the quantization problem would become more challenging. Since exact system parameters are often unknown for real systems, adaptive control is a useful approach to deal with such uncertainties, where an online estimation of the parameters can be provided. The work in [7], where a backstepping-based adaptive control scheme was presented, was further developed in [9] for the same stabilization problem to consider a hysteresis quantizer, that compared to a logarithmic quantizer has additional quantization levels to avoid chattering. Tracking control in the presence of input quantization has been considered in [10–13] for uncertain nonlinear systems, in [14] for a group of unmanned aerial vehicles with unknown parameters, in [15] for underactuated autonomous underwater vehicles (AUVs), in [16] for a 2 degrees-of-freedom (DOF) helicopter system. The developed methods in [5–16] all focused on the input quantization problem, while the controllers were designed by continuous measures of the state feedback.

Control of uncertain systems with state or output quantization has been studied in [17–20] using robust or adaptive approaches. In [17], an adaptive controller was developed for uncertain linear systems with quantized outputs. In [18], a robust controller for a linear multiple-input multiple-output (MIMO) uncertain system was designed with quantized output measurements. In [19], the stabilization problem for uncertain nonlinear systems with quantized states was investigated, and in [20], the attitude tracking control problem of rigid bodies with quantized states was considered, where in [19,20] adaptive backstepping-based control algorithms were designed.

Although research on quantized control has received much attention recent years, most work focus on either input or output quantization. In practice, the control signal sent to the actuator(s) and the signals sent from sensors to the control module

☆ This work was supported in part by IKTPLUSS DEEPCOBOT Project under Grant 306640/O70 from the Research Council of Norway.

* Corresponding author.
E-mail addresses: siri.schlanbusch@uia.no (S.M. Schlanbusch), jing.zhou@uia.no (J. Zhou).

https://doi.org/10.1016/j.sysconle.2023.105513

need to be quantized before transmitted due to the use of digital processors and considering the accuracy of sensors. Also, for remotely controlled systems, the control signals and sensor measurements are shared via a common digital network where the bandwidth might be limited and it is natural to suppose that both input and output signals are quantized. Some work that considered both input and state quantization are [21–27]. In [21], the quantization effects on remotely controlled single-input single-output (SISO) linear systems were studied, where the stabilization problem was transformed into a robust control problem. Sliding mode controllers were developed in [22,23] for trajectory tracking in the presence of both input and state quantization, of AUVs in [22], and of mechanical systems in [23]. Neural-network based adaptive tracking controllers in presence of quantization were designed in [24] for uncertain nonholonomic mobile robots, and in [25] for uncertain MIMO nonlinear systems. Adaptive backstepping based control schemes were developed in [26,27], where the attitude tracking control problem for uncertain rigid bodies was investigated in [26], and a class of uncertain nonlinear systems was considered in [27].

This paper investigates the attitude tracking control problem for a class of uncertain rigid body systems with quantization for both inputs and states. The system is modeled as a nonlinear MIMO system, with challenges in controller design due to its nonlinear behavior and uncertain parameters. A quantizer is used for the signals in order to reduce the communication burden, and a new adaptive backstepping based control scheme is developed to achieve tracking of a given reference signal, where the tracking error is shown to converge towards a residual. The proposed control scheme is implemented by experiments on a 2-DOF helicopter system. The main contributions of this paper are as follows.

- The attitude tracking control problem of uncertain nonlinear rigid body systems is investigated where both inputs and states are quantized. As far as we are concerned, this is the first paper that solves this problem with uncertain parameters and where both inputs and states are quantized by a class of quantizers, that satisfies the sector bounded property. A new adaptive backstepping-based controller is developed and a new approach to stability analysis is proposed. By choosing proper design parameters, all signals in the closed-loop system are ensured bounded and tracking is achieved.
- Note that some techniques are presented in [26] to handle the uniform quantization, where the quantization error is bounded by a constant. By contrast, a more general quantizer is considered in this paper. Since the quantization errors depend on the inputs of quantizers, they cannot be ensured bounded automatically. Several difficulties are introduced both in the control design and stability analysis for MIMO uncertain systems due to the fact that the quantization errors are not bounded by constants. Instead the quantization error is linearly dependent on the input to the quantizer, and is the main challenge to be handled. Other challenges:
  - Only the quantized states can be used to construct the control input and the virtual controller.
  - Since the virtual controllers are discontinuous after quantization, the derivative cannot be computed as is normally done in the standard backstepping procedure. To overcome the difficulty, differentiable virtual controls are designed by assuming that the system has no quantization. Their partial derivatives multiplied by the quantized signals are then utilized to complete the design of virtual controls.
  - The effects of both input and state quantization introduces several residual terms that need to be dominated.
- By well establishing the relations between the input signals and error states and functions of continuous signals and quantized signals, the stability of the closed-loop system equilibrium can be achieved by choosing proper design parameters.

2. Mathematical model and problem statement

2.1. Notations

Vectors are denoted by small bold letters and matrices with capitalized bold letters. The symbol $\boldsymbol{\omega}_{b,a}^{c}$ denotes angular velocity of frame a relative to frame b, expressed in frame c; $\boldsymbol{R}_{a}^{b}$ is the rotation matrix from frame a to frame b; the cross product operator $\times$ between two vectors $\boldsymbol{a}$ and $\boldsymbol{b}$ is written as $\boldsymbol{S}(\boldsymbol{a})\boldsymbol{b}$ where $\boldsymbol{S}$ is skew-symmetric; $\lambda_{\max}(\cdot)$ and $\lambda_{\min}(\cdot)$ denotes the maximum and minimum eigenvalue of the matrix $(\cdot)$, and $\|\cdot\|$ denotes the $\mathcal{L}_2$-norm and induced $\mathcal{L}_2$-norm for vectors and matrices, respectively.

2.2. Problem statement

For systems where data transmission are transferred through a common communication network, quantization errors are introduced due to the limited communication rate of the network. For low resolution, these errors cannot be ignored, and must be considered in the analysis and controller design since it will affect the performance and stability of the system.

We consider a control system as shown in Fig. 1, where the inputs $\boldsymbol{u}(t)$ and the states $\boldsymbol{\varepsilon}(t), \boldsymbol{\omega}(t)$ are quantized at the encoder side to be sent over a network. The network is assumed noiseless, so that the quantized signals $\boldsymbol{u}^{Q}(t), \boldsymbol{\varepsilon}^{Q}(t), \boldsymbol{\omega}^{Q}(t)$ are recovered after transmission.

The control problem is to design a control law by utilizing only quantized measurement of the states, so that tracking of a desired attitude is achieved.

2.3. Rigid body model

The orientation of a rigid body in frame b, relative to an inertial frame i, can be described by a unit quaternion [28–30], $\boldsymbol{q} = [\eta, \varepsilon_1, \varepsilon_2, \varepsilon_3]^\top = [\eta, \boldsymbol{\varepsilon}^\top]^\top \in \mathbb{S}^3 = \{\boldsymbol{x} \in \mathbb{R}^4 : \boldsymbol{x}^\top \boldsymbol{x} = 1\}$ that is a complex number, where $\eta = \cos(\upsilon/2) \in \mathbb{R}$ is the real part and $\boldsymbol{\varepsilon} = \boldsymbol{k}\sin(\upsilon/2) \in \mathbb{R}^3$ is the imaginary part, where υ is the Euler angle and $\boldsymbol{k}$ is the Euler axis, and $\mathbb{S}^3$ is the non-Euclidean three-sphere. The kinematic and dynamic equations for the rigid body are defined as

$$\dot{\boldsymbol{q}} = \boldsymbol{T}(\boldsymbol{q})\boldsymbol{\omega}, \tag{1}$$

$$\boldsymbol{J}\dot{\boldsymbol{\omega}} = -\boldsymbol{S}(\boldsymbol{\omega})(\boldsymbol{J}\boldsymbol{\omega}) + \Phi(\boldsymbol{\varepsilon}, \boldsymbol{\omega})^\top \boldsymbol{\theta} + \boldsymbol{u}^{Q}, \tag{2}$$

where the angular velocity $\boldsymbol{\omega}_{i,b}^{b} = \boldsymbol{\omega} \in \mathbb{R}^3$, the inertia matrix $\boldsymbol{J} \in \mathbb{R}^{3\times 3}$ is positive definite and invertible, the vector $\boldsymbol{\theta} \in \mathbb{R}^n$ is unknown and constant, the matrix $\Phi \in \mathbb{R}^{n\times 3}$ are known nonlinear functions, and where we have

$$\boldsymbol{T}(\boldsymbol{q}) = \frac{1}{2}\begin{bmatrix} -\boldsymbol{\varepsilon}^\top \\ \eta\boldsymbol{I} + \boldsymbol{S}(\boldsymbol{\varepsilon}) \end{bmatrix} \in \mathbb{R}^{4\times 3}. \tag{3}$$

The matrix $\boldsymbol{I}$ denotes the identity matrix and $\boldsymbol{S}(\cdot)$ is the skew-symmetric matrix given by

$$\boldsymbol{S}(\boldsymbol{\varepsilon}) = \begin{bmatrix} 0 & -\varepsilon_3 & \varepsilon_2 \\ \varepsilon_3 & 0 & -\varepsilon_1 \\ -\varepsilon_2 & \varepsilon_1 & 0 \end{bmatrix}. \tag{4}$$

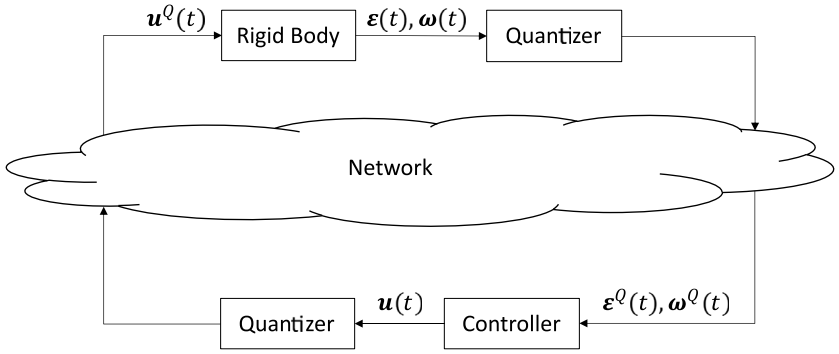

Fig. 1. Control system with input and state quantization over a network.

The orientation between two frames can be described by a rotation matrix given as

$$\boldsymbol{R}(\boldsymbol{q}) = \boldsymbol{I} + 2\eta \boldsymbol{S}(\boldsymbol{\varepsilon}) + 2\boldsymbol{S}^2(\boldsymbol{\varepsilon}), \tag{5}$$

where $\boldsymbol{R} \in SO(3)$ that is a special orthogonal group of order three, and has the property

$$SO(3) = \{\boldsymbol{R} \in \mathbb{R}^{3\times 3} : \boldsymbol{R}^\top \boldsymbol{R} = \boldsymbol{I}, \det(\boldsymbol{R}) = 1\}. \tag{6}$$

The mapping $\boldsymbol{R} : \mathbb{S}^3 \to SO(3)$ is everywhere a local diffeomorphism, but globally two-to-one, where $\boldsymbol{R}(\boldsymbol{q}) = \boldsymbol{R}(-\boldsymbol{q})$ [31]. The time derivative of a rotation matrix can be expressed as [30]

$$\dot{\boldsymbol{R}}_b^a = \boldsymbol{R}_b^a \boldsymbol{S}\left(\boldsymbol{\omega}_{a,b}^b\right) = \boldsymbol{S}\left(\boldsymbol{\omega}_{a,b}^a\right) \boldsymbol{R}_b^a. \tag{7}$$

Attitude and angular velocities are assumed to be measurable.

2.4. Quantizer

In this paper, we consider a class of quantizers satisfying the following inequality [32]

$$|y^Q - y| = |d| \le \delta |y| + y_{\min}, \tag{8}$$

where d is the quantization error, and $0 \le \delta < 1$ and $y_{\min} > 0$ are quantization parameters. If $\delta = 0$, the quantization error will only depend on $y_{\min}$, and so the quantization error is bounded by a constant. When $0 < \delta < 1$, the quantization error also depends on the input to the quantizer and is a sector bounded quantizer.

The quantized signals are modeled as

$$Q\left(\boldsymbol{u}(t)\right) = \boldsymbol{u}^Q(t), \tag{9}$$

$$Q(\boldsymbol{\varepsilon}(t)) = \boldsymbol{\varepsilon}^Q(t), \quad Q(\boldsymbol{\omega}(t)) = \boldsymbol{\omega}^Q(t), \tag{10}$$

where $Q(\cdot)$ is a quantizer, $\boldsymbol{u}(t) \in \mathbb{R}^3$ are the control inputs, $\boldsymbol{u}^Q(t) = [u_1^Q \; u_2^Q \; u_3^Q]^\top$ are the quantized inputs, $\boldsymbol{\varepsilon} \in \mathbb{R}^3$ and $\boldsymbol{\omega} \in \mathbb{R}^3$ are the measured states, and $\boldsymbol{\varepsilon}^Q(t) = [\varepsilon_1^Q \; \varepsilon_2^Q \; \varepsilon_3^Q]^\top$ and $\boldsymbol{\omega}^Q(t) = [\omega_1^Q \; \omega_2^Q \; \omega_3^Q]^\top$ are the quantized states, where each vector element satisfies (8) and so

$$\|\boldsymbol{u}^Q - \boldsymbol{u}\| = \|\boldsymbol{d}_u\| \le \|\boldsymbol{\delta}_u\| \, \|\boldsymbol{u}\| + \|\boldsymbol{u}_{\min}\| \triangleq \delta_u \|\boldsymbol{u}\| + u_{\min}, \tag{11}$$

$$\|\boldsymbol{\omega}^Q - \boldsymbol{\omega}\| = \|\boldsymbol{d}_\omega\| \le \|\boldsymbol{\delta}_\omega\| \, \|\boldsymbol{\omega}\| + \|\boldsymbol{\omega}_{\min}\| \triangleq \delta_\omega \|\boldsymbol{\omega}\| + \omega_{\min}, \tag{12}$$

$$\|\boldsymbol{\varepsilon}^Q - \boldsymbol{\varepsilon}\| = \|\boldsymbol{d}_\varepsilon\| \le \|\boldsymbol{\delta}_\varepsilon\| \, \|\boldsymbol{\varepsilon}\| + \|\boldsymbol{\varepsilon}_{\min}\| \le \|\boldsymbol{\delta}_\varepsilon\| + \|\boldsymbol{\varepsilon}_{\min}\| \triangleq \delta_\varepsilon, \tag{13}$$

where in (13), the unity property of the unit quaternion is used.

Most practical quantizers satisfy the property in (8), such as a uniform-, a logarithmic- and a logarithmic-uniform quantizer, and will be presented next.

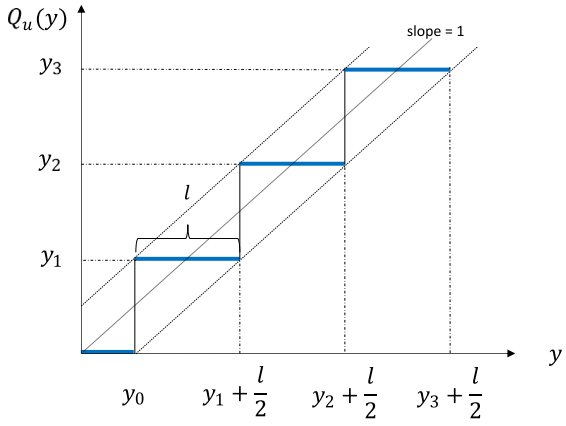

Fig. 2. Map of the uniform quantizer $Q_u(y)$ for $y > 0$.

2.4.1. Uniform quantizer

A uniform quantizer can be described as [33]

$$Q_u(y) = \begin{cases} y_i \operatorname{sgn}(y), & y_i - \frac{l}{2} < |y| \le y_i + \frac{l}{2} \\ 0, & |y| \le y_0 \end{cases}, \tag{14}$$

where $y_0 > 0$ and $y_1 = y_0 + \frac{l}{2}$, $y_i = y_{i-1} + l$ with $i = 2, 3, \ldots$, l is the length of the quantization interval and $\operatorname{sgn}(\cdot)$ is the sign function. The uniform quantization $Q_u(y)$ is in the set $U = \{0, \; \pm y_i\}$. The quantization error is bounded by a positive constant $y_{\min} = \max\{y_0, \; l/2\}$, and satisfies (8) with $\delta = 0$. A map of the uniform quantizer (14) for $y > 0$ is shown in Fig. 2. The uniform quantizer has equal quantization levels and is optimal for uniformly distributed signals.

2.4.2. Logarithmic quantizer

A logarithmic quantizer is defined as [33]

$$Q_{\log}(y) = \begin{cases} y_i \operatorname{sgn}(y), & \frac{y_i}{1+\delta} < |y| \le \frac{y_i}{1-\delta} \\ 0, & |y| \le y_{\min}, \end{cases} \tag{15}$$

where $y_{\min} = \frac{y_0}{1+\delta}$ determines the size of the dead-zone for $Q_{\log}(y)$, $0 < \delta < 1$, $y_0 > 0$, $y_i = \rho^{(1-i)} y_0$, with $i = 1, 2, \ldots$, and parameter $\rho = \frac{1-\delta}{1+\delta}$. The parameter ρ can be regarded as a measure of the quantization density, where smaller values of ρ implies that the quantizer is coarser. The quantized signal $Q_{\log}(y)$ is in the set $U = \{0, \; \pm y_i\}$ and satisfies the property in (8). A map of the logarithmic quantizer (15) for $y > 0$ is shown in Fig. 3. The logarithmic quantizer has unequal quantization levels, and is useful where the signals are more concentrated near the equilibrium

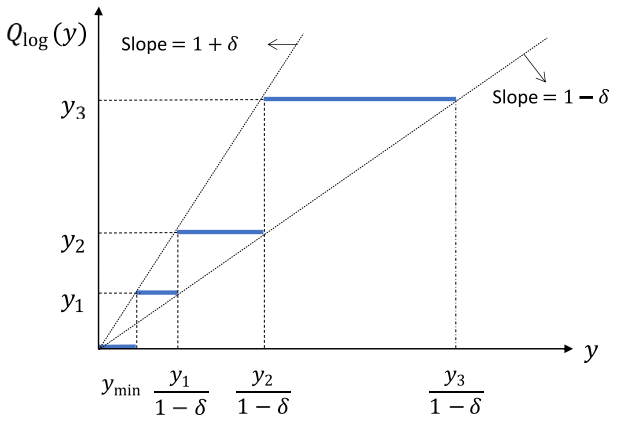

Fig. 3. Map of the logarithmic quantizer $Q_{\log}(y)$ for $y > 0$.

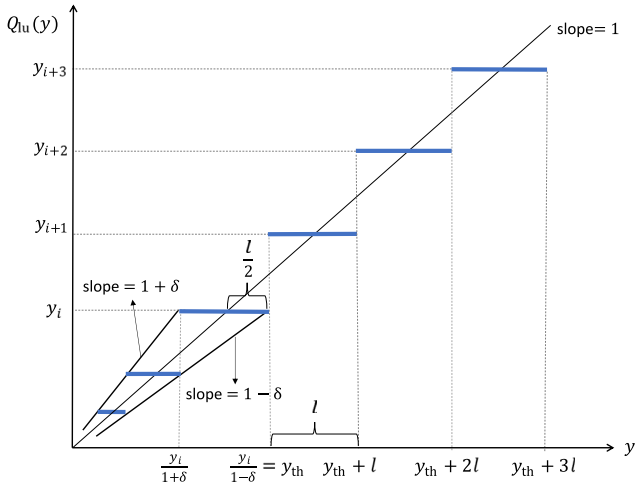

Fig. 4. Map of the logarithmic-uniform quantizer $Q_{\text{lu}}(y)$ for $y > 0$.

or have higher resolution around the equilibrium, e.g. for speech signal compression, image processing, etc. Several remarks about the logarithmic quantizer can be found in [7,34,35].

2.4.3. Logarithmic-uniform quantizer

A logarithmic-uniform quantizer combines a uniform quantizer and a logarithmic quantizer and is defined as [32]

$$Q_{\text{lu}}(y) = \begin{cases} Q_{\log}(y_{\text{th}}) + Q_u(y - y_{\text{th}}), & |y| \geq y_{\text{th}} \\ Q_{\log}(y) & |y| < y_{\text{th}} \end{cases}, \tag{16}$$

where y_{th} is a positive constant specified by designer denoting the threshold to switch between the logarithmic and uniform quantizer. The uniform quantizer, Q_u, is defined in (14) and the logarithmic quantizer, $Q_{\log}$, is defined in (15). The quantizer $Q_{\text{lu}}(y)$ takes advantage of a logarithmic quantizer having high resolution close to the origin, and switch to a uniform quantizer for higher values, and satisfies (8) with $\delta = 0$ and $y_{\min} \geq \frac{l}{2}$. A map of the logarithmic-uniform quantizer (16) for $y > 0$ is shown in Fig. 4.

2.5. Control objective

We want to track a given desired attitude $\boldsymbol{q}_{i,d} = \boldsymbol{q}_d$ and a desired angular velocity $\boldsymbol{\omega}_{i,d}^i = \boldsymbol{\omega}_d$ where the kinematic equation

$$\dot{\boldsymbol{q}}_d = \boldsymbol{T}(\boldsymbol{q}_d)\boldsymbol{\omega}_{i,d}^d = \frac{1}{2}\begin{bmatrix} -\boldsymbol{\varepsilon}_d^\top \\ \eta_d \boldsymbol{I} - \boldsymbol{S}(\boldsymbol{\varepsilon}_d) \end{bmatrix} \boldsymbol{\omega}_d, \tag{17}$$

is satisfied. The tracking error $\boldsymbol{e}$, is given by the quaternion product

$$\boldsymbol{e} = \bar{\boldsymbol{q}}_{i,d} \otimes \boldsymbol{q}_{i,b} = \begin{bmatrix} \tilde{\eta} \\ \tilde{\boldsymbol{\varepsilon}} \end{bmatrix} = \begin{bmatrix} \eta_d \eta + \boldsymbol{\varepsilon}_d^\top \boldsymbol{\varepsilon} \\ \eta_d \boldsymbol{\varepsilon} - \eta \boldsymbol{\varepsilon}_d - S(\boldsymbol{\varepsilon}_d)\boldsymbol{\varepsilon} \end{bmatrix} \in \mathbb{S}^3, \tag{18}$$

where $\bar{\boldsymbol{q}} = [\eta \quad -\boldsymbol{\varepsilon}^\top]^\top$ is the inverse rotation given by the complex conjugate. If $\boldsymbol{q}_{i,b} = \boldsymbol{q}_{i,d}$, then $\boldsymbol{e} = [\pm 1 \ \boldsymbol{0}_3^\top]^\top$ where $\boldsymbol{0}_3$ is the zero vector of dimension three. Since there exist two equilibria using the quaternion representation, we conclude that global stability cannot be achieved. Physically $\boldsymbol{e}$ and $-\boldsymbol{e}$ represent the same attitude, only rotated $\pm 2\pi$ about an axis relative to each other, but mathematically the two equilibria are distinct.

The relative error kinematics is

$$\dot{\boldsymbol{e}} = \boldsymbol{T}(\boldsymbol{e})\boldsymbol{\omega}_e, \tag{19}$$

where $\boldsymbol{T}(\cdot)$ is defined in (3), and the angular velocity error

$$\boldsymbol{\omega}_e = \boldsymbol{\omega} - \boldsymbol{R}_i^b \boldsymbol{\omega}_d. \tag{20}$$

The control objective is to design a control law for $\boldsymbol{u}(t) = \boldsymbol{u}(\boldsymbol{\varepsilon}^{\mathrm{Q}}, \boldsymbol{\omega}^{\mathrm{Q}})$ by utilizing only the quantized states $\boldsymbol{\varepsilon}^{\mathrm{Q}}$ and $\boldsymbol{\omega}^{\mathrm{Q}}$ to drive $\tilde{\boldsymbol{\varepsilon}}$ and $\boldsymbol{\omega}_e$ towards zero and where all the signals in the closed-loop system are uniformly bounded. To achieve the objective, the following assumptions are imposed.

Assumption 1. The desired attitude, angular velocity and angular acceleration, $\boldsymbol{q}_d(t)$, $\boldsymbol{\omega}_d(t)$ and $\dot{\boldsymbol{\omega}}_d(t)$ are known, piecewise continuous and bounded, where $\| \boldsymbol{\omega}_d(t)\| < k_{\omega_d}$ and $\| \dot{\boldsymbol{\omega}}_d(t)\| < k_{\dot{\omega}_d} \ \ \forall t \geq t_0$ where $k_{\omega_d}, k_{\dot{\omega}_d} > 0$.

Assumption 2. The unknown parameter vector $\boldsymbol{\theta}$ is bounded by $\|\boldsymbol{\theta}\| \leq k_\theta$, where k_θ is a positive constant. Also $\boldsymbol{\theta} \in C_\theta$, where C_θ is a known compact convex set.

Assumption 3. The function Φ satisfy a locally Lipschitz condition such that

$$\|\Phi(\boldsymbol{x}_1, \boldsymbol{y}_1) - \Phi(\boldsymbol{x}_2, \boldsymbol{y}_2)\| \leq L_1\|\boldsymbol{x}_1 - \boldsymbol{x}_2\| + L_2\|\boldsymbol{y}_1 - \boldsymbol{y}_2\|, \tag{21}$$

where L_1 and L_2 are positive constants, and $\boldsymbol{x}_{(\cdot)}, \boldsymbol{y}_{(\cdot)} \in \mathbb{R}^3$ are real vectors.

Assumption 4. $\operatorname{sgn}(\tilde{\eta}(t_0)) = \operatorname{sgn}(\tilde{\eta}(t)) \ \ \forall t \geq t_0$.

Remark 1. These assumptions are reasonable for most practical systems. Assumption 1 ensures that the reference signal is bounded in t, and is a standard condition for attitude tracking control problems, see e.g [36–38]. Since the vector $\boldsymbol{\theta}$ has constant vector elements, Assumption 2 holds, knowing the bounds for each vector element. Assumption 3 is a fairly mild assumption to ensure the existence and uniqueness of solutions for the system (2) and applies for a broad class of practical systems, where similar assumptions are made in e.g [19,27]. By Assumption 4, the equilibrium point that initially are closest is chosen and kept throughout the tracking maneuver.

3. Controller design

In this section we will design adaptive feedback control laws for the rigid body using backstepping technique in [39]. Since the design of an adaptive controller with quantized signals is based on the design with continuous measurement of the signals, we start by the case of continuous signals before proceeding to the case of quantized signals.

3.1. Continuous signals

We here consider the case that the signals are not quantized. First, introducing a change of coordinates

$$\boldsymbol{z}_{1\pm} = \begin{bmatrix} 1 \mp \tilde{\eta} \\ \tilde{\boldsymbol{\varepsilon}} \end{bmatrix}, \tag{22}$$

$$\boldsymbol{z}_2 = \boldsymbol{\omega}_e - \boldsymbol{\alpha}, \tag{23}$$

where $\boldsymbol{z}_{1\pm}$ is an error vector, which shifts the equilibria to the origin [40], where $\boldsymbol{z}_{1+}$ is for the positive equilibrium point when $\tilde{\eta}(t_0) \geq 0$, and $\boldsymbol{z}_{1-}$ is for the negative equilibrium point when $\tilde{\eta}(t_0) < 0$, and where $\boldsymbol{\alpha}$ is a virtual controller chosen as

$$\boldsymbol{\alpha} = -\boldsymbol{C}_1 \boldsymbol{G} \boldsymbol{z}_{1\pm} \in \mathbb{R}^3, \tag{24}$$

where $\boldsymbol{C}_1 \in \mathbb{R}^{3\times 3}$ is a positive definite matrix and

$$\boldsymbol{G}(\boldsymbol{e})^\top \triangleq \begin{bmatrix} \pm\tilde{\boldsymbol{\varepsilon}}^\top \\ \tilde{\eta}\boldsymbol{I} + \boldsymbol{S}(\tilde{\boldsymbol{\varepsilon}}) \end{bmatrix} \in \mathbb{R}^{4\times 3}. \tag{25}$$

Remark 2. By introducing the change of coordinates $\boldsymbol{z}_{1\pm}$ we are avoiding that one of the mathematical representations of a given attitude is left unstable. The initial condition of $\tilde{\eta}$ given by Assumption 4 is also helpful in the control strategy, where we choose a target equilibrium point before we start the maneuver. If we were considering that only one of the equilibria was stable, the other would be unstable. Then, if we initially were close to the unstable equilibrium point, we would need a large rotation to reach the stable equilibrium point. We are thus avoiding the problem of unwinding since we now are regulating towards the closest equilibrium point, i.e the equilibrium point which requires the shortest rotation and thus minimizing the path length.

Remark 3. By choosing a target equilibrium point prior to the maneuver we will minimize the path length, but not necessarily the input energy. If there is an initial velocity in the opposite direction to the desired rotation it might be more efficient to converge towards the equilibrium that is further away to save energy [40].

For ease of notation we now denote $\boldsymbol{z}_1 = \boldsymbol{z}_{1\pm}$. The derivative of (22)–(23), inserting the dynamics from (2) is given as

$$\dot{\boldsymbol{z}}_1 = \frac{1}{2}\boldsymbol{G}^\top \boldsymbol{\omega}_e = -\frac{1}{2}\boldsymbol{G}^\top \boldsymbol{C}_1 \boldsymbol{G} \boldsymbol{z}_1 + \frac{1}{2}\boldsymbol{G}^\top \boldsymbol{z}_2, \tag{26}$$

$$\boldsymbol{J}\dot{\boldsymbol{z}}_2 = -\boldsymbol{S}(\boldsymbol{\omega})(\boldsymbol{J}\boldsymbol{\omega}) + \boldsymbol{\Phi}^\top \boldsymbol{\theta} + \boldsymbol{u}^{\mathrm{Q}} + \boldsymbol{J}\left(\boldsymbol{S}(\boldsymbol{\omega})\boldsymbol{R}_i^b \boldsymbol{\omega}_d - \boldsymbol{R}_i^b \dot{\boldsymbol{\omega}}_d - \dot{\boldsymbol{\alpha}}\right), \tag{27}$$

where the derivative of (24) is

$$\dot{\boldsymbol{\alpha}} = \mp\frac{1}{2}\boldsymbol{C}_1 \left[\tilde{\eta}\boldsymbol{I} + \boldsymbol{S}(\tilde{\boldsymbol{\varepsilon}})\right] \boldsymbol{\omega}_e, \tag{28}$$

where we have used that $\boldsymbol{G}\boldsymbol{z}_1 = \pm\tilde{\boldsymbol{\varepsilon}}$. Since the inputs are not quantized, we have $\boldsymbol{u}^{\mathrm{Q}} = \boldsymbol{u}$, and an adaptive controller and parameter update law can be designed as

$$\begin{aligned} \boldsymbol{u} = &-\boldsymbol{G}\boldsymbol{z}_1 - \boldsymbol{C}_2 \boldsymbol{z}_2 - \boldsymbol{\Phi}^\top \hat{\boldsymbol{\theta}} + \boldsymbol{S}(\boldsymbol{R}_i^b \boldsymbol{\omega}_d)(\boldsymbol{J}\boldsymbol{\omega}) \\ &+ \boldsymbol{S}(\boldsymbol{\alpha})(\boldsymbol{J}\boldsymbol{\omega}) - \boldsymbol{J}\left(\boldsymbol{S}(\boldsymbol{\omega})\boldsymbol{R}_i^b \boldsymbol{\omega}_d - \boldsymbol{R}_i^b \dot{\boldsymbol{\omega}}_d - \dot{\boldsymbol{\alpha}}\right), \end{aligned} \tag{29}$$

$$\dot{\hat{\boldsymbol{\theta}}} = \boldsymbol{\Gamma}\boldsymbol{\Phi}\boldsymbol{z}_2, \tag{30}$$

where $\boldsymbol{C}_2 \in \mathbb{R}^{3\times 3}, \boldsymbol{\Gamma} \in \mathbb{R}^{n\times n}$ are positive definite matrices, and the vector $\hat{\boldsymbol{\theta}}$ is the estimated value of $\boldsymbol{\theta}$. A Lyapunov function candidate is chosen as

$$V(\boldsymbol{z}_1, \boldsymbol{z}_2, \tilde{\boldsymbol{\theta}}, t) = \boldsymbol{z}_1^\top \boldsymbol{z}_1 + \frac{1}{2}\boldsymbol{z}_2^\top \boldsymbol{J}\boldsymbol{z}_2 + \frac{1}{2}\tilde{\boldsymbol{\theta}}^\top \boldsymbol{\Gamma}^{-1}\tilde{\boldsymbol{\theta}}, \tag{31}$$

where $\tilde{\boldsymbol{\theta}} = \boldsymbol{\theta} - \hat{\boldsymbol{\theta}}$ is the unknown parameter error. By inserting (29)–(30) in the derivative of (31) yields

$$\begin{aligned} \dot{V} &= -\boldsymbol{z}_1^\top \boldsymbol{G}^\top \boldsymbol{C}_1 \boldsymbol{G} \boldsymbol{z}_1 + \boldsymbol{z}_1^\top \boldsymbol{G}^\top \boldsymbol{z}_2 + \boldsymbol{z}_2^\top \left[-\boldsymbol{S}(\boldsymbol{\omega})(\boldsymbol{J}\boldsymbol{\omega}) + \boldsymbol{\Phi}^\top \boldsymbol{\theta} + \boldsymbol{u} \right. \\ &\quad \left. + \boldsymbol{J}\left(\boldsymbol{S}(\boldsymbol{\omega})\boldsymbol{R}_i^b \boldsymbol{\omega}_d - \boldsymbol{R}_i^b \dot{\boldsymbol{\omega}}_d - \dot{\boldsymbol{\alpha}}\right)\right] - \tilde{\boldsymbol{\theta}}^\top \boldsymbol{\Gamma}^{-1}\dot{\hat{\boldsymbol{\theta}}} \\ &= -\boldsymbol{z}_1^\top \boldsymbol{G}^\top \boldsymbol{C}_1 \boldsymbol{G} \boldsymbol{z}_1 - \boldsymbol{z}_2^\top \left[\boldsymbol{S}(\boldsymbol{\omega} - \boldsymbol{\alpha} - \boldsymbol{R}_i^b \boldsymbol{\omega}_d)(\boldsymbol{J}\boldsymbol{\omega})\right] - \boldsymbol{z}_2^\top \boldsymbol{C}_2 \boldsymbol{z}_2 \\ &= -\boldsymbol{z}_1^\top \boldsymbol{G}^\top \boldsymbol{C}_1 \boldsymbol{G} \boldsymbol{z}_1 - \boldsymbol{z}_2^\top \boldsymbol{C}_2 \boldsymbol{z}_2, \end{aligned} \tag{32}$$

where we have used the fact that $\boldsymbol{z}_2^\top \boldsymbol{S}(\boldsymbol{z}_2) = 0$. Then it follows that asymptotic tracking is achieved and all signals in the closed-loop system are uniformly bounded.

3.2. Quantized signals

Now we consider the case that both the inputs and the states are quantized, and satisfy the sector bounded property in (8). Since only the quantized states $\boldsymbol{\varepsilon}^{\mathrm{Q}}, \boldsymbol{\omega}^{\mathrm{Q}}$ are measured, the quantized value of η is calculated as

$$\eta^{\mathrm{Q}} = \pm\sqrt{1 - (\boldsymbol{\varepsilon}^{\mathrm{Q}})^\top \boldsymbol{\varepsilon}^{\mathrm{Q}}}, \tag{33}$$

where the quantized attitude is given by $\boldsymbol{q}^{\mathrm{Q}} = [\eta^{\mathrm{Q}}, (\boldsymbol{\varepsilon}^{\mathrm{Q}})^\top]^\top$.

Remark 4. The value of η^{Q} can be calculated based on the value of $\boldsymbol{\varepsilon}^{\mathrm{Q}}$ and knowledge of the sign of $\eta(t_0)$ and the assumption of sign continuity of $\eta(t)$ based on derivative. If we are close to, or at $\eta = 0$, we might end up with $(\boldsymbol{\varepsilon}^{\mathrm{Q}})^\top \boldsymbol{\varepsilon}^{\mathrm{Q}} > 1$, and a scaling is needed to ensure we have a unit quaternion.

The quantization error of the quaternion can be expressed as

$$\boldsymbol{d}_q = \bar{\boldsymbol{q}}_{i,b} \otimes \boldsymbol{q}_{i,\mathrm{Q}} = \begin{bmatrix} d_\eta \\ \boldsymbol{d}_{\tilde{\varepsilon}} \end{bmatrix} = \begin{bmatrix} \eta\eta^{\mathrm{Q}} + \boldsymbol{\varepsilon}^\top \boldsymbol{\varepsilon}^{\mathrm{Q}} \\ \eta\boldsymbol{\varepsilon}^{\mathrm{Q}} - \eta^{\mathrm{Q}}\boldsymbol{\varepsilon} - S(\boldsymbol{\varepsilon})\boldsymbol{\varepsilon}^{\mathrm{Q}} \end{bmatrix}, \tag{34}$$

where $\boldsymbol{d}_{\tilde{\varepsilon}}$ is bounded by $\|\boldsymbol{d}_{\tilde{\varepsilon}}\| \leq k_\varepsilon \delta_\varepsilon$ from (13) and where $k_\varepsilon > 1$ is a positive constant, and d_η is bounded from the unity property of unit quaternion. If $\boldsymbol{q}^{\mathrm{Q}} = \boldsymbol{q}$ and there is no quantization error, then $\boldsymbol{d}_q = [1\ 0\ 0\ 0]^\top$. The tracking error with the quantized value of the unit quaternion is given by

$$\boldsymbol{e}^{\mathrm{Q}} = \begin{bmatrix} \tilde{\eta}^{\mathrm{Q}} \\ \tilde{\boldsymbol{\varepsilon}}^{\mathrm{Q}} \end{bmatrix} = \begin{bmatrix} \eta_d \eta^{\mathrm{Q}} + \boldsymbol{\varepsilon}_d^\top \boldsymbol{\varepsilon}^{\mathrm{Q}} \\ \eta_d \boldsymbol{\varepsilon}^{\mathrm{Q}} - \eta^{\mathrm{Q}}\boldsymbol{\varepsilon}_d - S(\boldsymbol{\varepsilon}_d)\boldsymbol{\varepsilon}^{\mathrm{Q}} \end{bmatrix}, \tag{35}$$

and can also be described by

$$\boldsymbol{e}^{\mathrm{Q}} = \boldsymbol{q}_{d,b} \otimes \boldsymbol{q}_{b,\mathrm{Q}} = \boldsymbol{e} \otimes \boldsymbol{d}_q \triangleq \begin{bmatrix} \tilde{\eta}^{\mathrm{Q}} \\ \tilde{\boldsymbol{\varepsilon}} + \boldsymbol{d}_{\tilde{\varepsilon}} \end{bmatrix}, \tag{36}$$

where the value of $\boldsymbol{d}_{\tilde{\varepsilon}}$ depends on the quantization error that is bounded by (13), and if there is no quantization error, $\boldsymbol{d}_{\tilde{\varepsilon}} = \boldsymbol{0}$. The adaptive controller and parameter update law are designed as

$$\boldsymbol{u}^{\mathrm{Q}}(t) = \boldsymbol{u}(t) + \boldsymbol{d}_u(t), \tag{37}$$

$$\begin{aligned} \boldsymbol{u} = &-\boldsymbol{G}^{\mathrm{Q}}\boldsymbol{z}_1^{\mathrm{Q}} - \boldsymbol{C}_2 \boldsymbol{z}_2^{\mathrm{Q}} - (\boldsymbol{\Phi}^{\mathrm{Q}})^\top \hat{\boldsymbol{\theta}} + \boldsymbol{S}(\boldsymbol{R}_i^{\mathrm{Q}} \boldsymbol{\omega}_d)(\boldsymbol{J}\boldsymbol{\omega}^{\mathrm{Q}}) \\ &+ \boldsymbol{S}(\boldsymbol{\alpha}^{\mathrm{Q}})(\boldsymbol{J}\boldsymbol{\omega}^{\mathrm{Q}}) - \boldsymbol{J}\left(\boldsymbol{S}(\boldsymbol{\omega}^{\mathrm{Q}})\boldsymbol{R}_i^{\mathrm{Q}} \boldsymbol{\omega}_d - \boldsymbol{R}_i^{\mathrm{Q}} \dot{\boldsymbol{\omega}}_d - \tilde{\boldsymbol{\alpha}}^{\mathrm{Q}}\right), \end{aligned} \tag{38}$$

$$\dot{\hat{\boldsymbol{\theta}}} = \mathrm{Proj}\{\boldsymbol{\Gamma}\boldsymbol{\Phi}^{\mathrm{Q}}\boldsymbol{z}_2^{\mathrm{Q}}\}, \tag{39}$$

where Proj$\{\cdot\}$ is the projection operator given in [39] and where

$$\boldsymbol{z}_1^{\mathrm{Q}} = \begin{bmatrix} 1 \mp \tilde{\eta}^{\mathrm{Q}} \\ \tilde{\boldsymbol{\varepsilon}}^{\mathrm{Q}} \end{bmatrix}, \tag{40}$$

$$\boldsymbol{z}_2^{\mathrm{Q}} = \boldsymbol{\omega}_e^{\mathrm{Q}} - \boldsymbol{\alpha}^{\mathrm{Q}}, \tag{41}$$

$$\boldsymbol{G}(\boldsymbol{e}^{\mathrm{Q}})^\top = \begin{bmatrix} \pm(\tilde{\boldsymbol{\varepsilon}}^{\mathrm{Q}})^\top \\ \tilde{\eta}^{\mathrm{Q}}\boldsymbol{I} + \boldsymbol{S}(\tilde{\boldsymbol{\varepsilon}}^{\mathrm{Q}}) \end{bmatrix}, \tag{42}$$

$$\boldsymbol{\alpha}^{\mathrm{Q}} = -\boldsymbol{C}_1 \boldsymbol{G}^{\mathrm{Q}} \boldsymbol{z}_1^{\mathrm{Q}} = \mp\boldsymbol{C}_1 \tilde{\boldsymbol{\varepsilon}}^{\mathrm{Q}}, \tag{43}$$

$$\boldsymbol{\Phi}^{\mathrm{Q}} = \boldsymbol{\Phi}(\boldsymbol{\varepsilon}^{\mathrm{Q}}, \boldsymbol{\omega}^{\mathrm{Q}}), \tag{44}$$

$$\bar{\boldsymbol{\alpha}}^{\mathrm{Q}} \triangleq \mp\frac{1}{2}\boldsymbol{C}_1\left[\tilde{\eta}^{\mathrm{Q}}\boldsymbol{I} + \boldsymbol{S}(\tilde{\boldsymbol{\varepsilon}}^{\mathrm{Q}})\right]\boldsymbol{\omega}_e^{\mathrm{Q}}, \tag{45}$$

$$\boldsymbol{\omega}_e^{\mathrm{Q}} = \boldsymbol{\omega}^{\mathrm{Q}} - \boldsymbol{R}_i^{\mathrm{Q}}\boldsymbol{\omega}_d, \tag{46}$$

$$\boldsymbol{R}_i^{\mathrm{Q}} = \boldsymbol{R}_b^{\mathrm{Q}}\boldsymbol{R}_i^b, \tag{47}$$

where $\boldsymbol{R}_b^{\mathrm{Q}}$ is the rotation due to the quantization error. The projection operator is ensuring that the estimates are nonzero and within known bounds, that is $\|\hat{\boldsymbol{\theta}}\| \leq k_\theta$. A function $\bar{\boldsymbol{\alpha}}^{\mathrm{Q}}$ is used in (45), which is designed as if the states were not quantized. See e.g. [remark 7] in [19] for a note about this design.

4. Stability analysis

To analyze the closed-loop stability, we first establish some preliminary results as stated in the following Lemmas, and with proofs provided in Appendix A–Appendix D, respectively. The results in this section are applicable for the quantizers satisfying the sector bounded property in (8), including the uniform quantizer in Section 2.4.1, the logarithmic quantizer in Section 2.4.2, and the logarithmic-uniform quantizer in Section 2.4.3.

Lemma 1. *The virtual control law $\boldsymbol{\alpha}$, the output $\boldsymbol{\omega}$ and angular velocity error $\boldsymbol{\omega}_e$ are bounded by the following inequalities:*

$$\|\boldsymbol{\alpha}\| \leq \lambda_{\max}(\boldsymbol{C}_1), \tag{48}$$

$$\|\boldsymbol{\omega}_e\| \leq \lambda_{\max}(\boldsymbol{C}_1) + \|\boldsymbol{z}\|, \tag{49}$$

$$\|\boldsymbol{\omega}\| \leq k_\omega + \|\boldsymbol{z}\|, \tag{50}$$

where $\boldsymbol{z} = [\boldsymbol{z}_1^\top, \boldsymbol{z}_2^\top]^\top$, and

$$k_\omega \triangleq \lambda_{\max}(\boldsymbol{C}_1) + k_{\omega_d}. \tag{51}$$

Lemma 2. *The effects of state quantization are bounded by the following inequalities:*

$$\text{(i)}\ \|\boldsymbol{R}_i^{\mathrm{Q}} - \boldsymbol{R}_i^b\| \leq \delta_\varepsilon k_R, \tag{52}$$

$$\text{(ii)}\ \|\boldsymbol{G}^{\mathrm{Q}}\boldsymbol{z}_1^{\mathrm{Q}} - \boldsymbol{G}\boldsymbol{z}_1\| \leq \delta_\varepsilon k_\varepsilon, \tag{53}$$

$$\text{(iii)}\ \|\boldsymbol{\alpha}^{\mathrm{Q}} - \boldsymbol{\alpha}\| \leq \delta_\varepsilon k_\alpha, \tag{54}$$

$$\text{(iv)}\ \|\boldsymbol{\omega}^{\mathrm{Q}} - \boldsymbol{\omega}\| \leq \delta_\omega k_\omega + \omega_{\min} + \delta_\omega\|\boldsymbol{z}\|, \tag{55}$$

$$\text{(v)}\ \|\boldsymbol{\omega}_e^{\mathrm{Q}} - \boldsymbol{\omega}_e\| \leq \delta_\varepsilon k_R k_{\omega_d} + \delta_\omega k_\omega + \omega_{\min} + \delta_\omega\|\boldsymbol{z}\|, \tag{56}$$

$$\text{(vi)}\ \|\boldsymbol{z}_2^{\mathrm{Q}} - \boldsymbol{z}_2\| \leq \delta_\varepsilon k_{z_2} + \delta_\omega k_\omega + \omega_{\min} + \delta_\omega\|\boldsymbol{z}\|, \tag{57}$$

$$\text{(vii)}\ \|\bar{\boldsymbol{\alpha}}^{\mathrm{Q}} - \dot{\boldsymbol{\alpha}}\| \leq \delta_\varepsilon k_{\bar{\alpha}_1} + \delta_\omega k_{\bar{\alpha}_2} + \omega_{\min} k_{\bar{\alpha}_3} + \lambda_{\max}(\boldsymbol{C}_1)^2 + (\lambda_{\max}(\boldsymbol{C}_1) + \delta_\omega)\|\boldsymbol{z}\|, \tag{58}$$

$$\text{(viii)}\ \|\Phi^{\mathrm{Q}} - \Phi\| \leq \delta_\varepsilon L_1 + \delta_\omega L_2 k_\omega + \omega_{\min} L_2 + \delta_\omega L_2\|\boldsymbol{z}\|, \tag{59}$$

where

$$k_R \triangleq 2k_\varepsilon + 2k_\varepsilon^2\delta_\varepsilon, \tag{60}$$

$$k_\alpha \triangleq \lambda_{\max}(\boldsymbol{C}_1)k_\varepsilon, \tag{61}$$

$$k_{z_2} \triangleq k_R k_{\omega_d} + k_\alpha, \tag{62}$$

$$k_{\bar{\alpha}_1} \triangleq \frac{1}{2}\lambda_{\max}(\boldsymbol{C}_1)k_R k_{\omega_d}, \tag{63}$$

$$k_{\bar{\alpha}_2} \triangleq \frac{1}{2}\lambda_{\max}(\boldsymbol{C}_1)k_\omega, \tag{64}$$

$$k_{\bar{\alpha}_3} \triangleq \frac{1}{2}\lambda_{\max}(\boldsymbol{C}_1), \tag{65}$$

are positive constants.

Lemma 3. *The effect of input quantization is bounded by the following inequality:*

$$\|\boldsymbol{u}^{\mathrm{Q}} - \boldsymbol{u}\| \leq \delta_u\left(\delta_\varepsilon k_{u_1} + \delta_\omega k_{u_2} + \omega_{\min} k_{u_3} + k_{u_4}\right) + u_{\min} + \delta_u\left(\delta_\varepsilon k_{u_5} + \delta_\omega k_{u_6} + k_{u_7}\right)\|\boldsymbol{z}\|, \tag{66}$$

where

$$k_{u_1} \triangleq k_\varepsilon + \lambda_{\max}(\boldsymbol{C}_2)k_{z_2} + k_\theta L_1 + \lambda_{\max}(\boldsymbol{J})k_\alpha\left(\delta_\omega k_\omega + \omega_{\min} + k_\omega\right) + \lambda_{\max}(\boldsymbol{J})k_{\bar{\alpha}_1}, \tag{67}$$

$$k_{u_2} \triangleq \lambda_{\max}(\boldsymbol{C}_2)k_\omega + L_2 k_\omega k_\theta + \lambda_{\max}(\boldsymbol{J})\left(2k_{\omega_d}k_\omega + \lambda_{\max}(\boldsymbol{C}_1)k_\omega + k_{\bar{\alpha}_2}\right), \tag{68}$$

$$k_{u_3} \triangleq \lambda_{\max}(\boldsymbol{C}_2) + L_2 k_\theta + \lambda_{\max}(\boldsymbol{J})\left(2k_{\omega_d} + \lambda_{\max}(\boldsymbol{C}_1) + k_{\bar{\alpha}_3}\right), \tag{69}$$

$$k_{u_4} \triangleq 1 + k_\theta\left(1 + k_\omega\right) + \lambda_{\max}(\boldsymbol{J})\left(2k_{\omega_d}k_\omega + \lambda_{\max}(\boldsymbol{C}_1)k_\omega + k_{\dot{\omega}_d}\right) + \frac{3}{2}\lambda_{\max}(\boldsymbol{J})\lambda_{\max}(\boldsymbol{C}_1)^2, \tag{70}$$

$$k_{u_5} \triangleq \lambda_{\max}(\boldsymbol{J})k_\alpha, \tag{71}$$

$$k_{u_6} \triangleq \lambda_{\max}(\boldsymbol{C}_2) + L_2 k_\theta + \lambda_{\max}(\boldsymbol{J})\left(2k_{\omega_d} + \delta_\varepsilon k_\alpha + \lambda_{\max}(\boldsymbol{C}_1) + 1\right), \tag{72}$$

$$k_{u_7} \triangleq \lambda_{\max}(\boldsymbol{C}_2) + k_\theta + \lambda_{\max}(\boldsymbol{J})\left(2k_{\omega_d} + \frac{5}{4}\lambda_{\max}(\boldsymbol{C}_1)\right), \tag{73}$$

are positive constants.

Lemma 4. *The following inequality holds:*

$$\frac{1}{2}\lambda_{\min}(\boldsymbol{C}_1)\boldsymbol{z}_1^\top\boldsymbol{z}_1 \leq \boldsymbol{z}_1^\top\boldsymbol{G}^\top\boldsymbol{C}_1\boldsymbol{G}\boldsymbol{z}_1. \tag{74}$$

By using the properties of Lemmas 1 and 2, we can show the following inequalities,

$$\begin{aligned}
&\boldsymbol{S}(\boldsymbol{\omega})(\boldsymbol{J}\boldsymbol{\omega}) - \boldsymbol{S}(\boldsymbol{R}_i^{\mathrm{Q}}\boldsymbol{\omega}_d)(\boldsymbol{J}\boldsymbol{\omega}^{\mathrm{Q}}) - \boldsymbol{S}(\boldsymbol{\alpha}^{\mathrm{Q}})(\boldsymbol{J}\boldsymbol{\omega}^{\mathrm{Q}}) \\
&\leq \boldsymbol{S}(\boldsymbol{\omega})(\boldsymbol{J}\boldsymbol{\omega}) - \boldsymbol{S}(\boldsymbol{R}_i^b\boldsymbol{\omega}_d)(\boldsymbol{J}\boldsymbol{\omega}) - \boldsymbol{S}(\boldsymbol{\alpha})(\boldsymbol{J}\boldsymbol{\omega}) \\
&\quad + \lambda_{\max}(\boldsymbol{J})\left[(\delta_\varepsilon k_R k_{\omega_d} + \delta_\varepsilon k_\alpha)\|\boldsymbol{\omega}^{\mathrm{Q}}\| + (k_{\omega_d} + \|\boldsymbol{\alpha}\|)\|\boldsymbol{d}_\omega\|\right] \\
&\leq \boldsymbol{S}(\boldsymbol{z}_2)(\boldsymbol{J}\boldsymbol{\omega}) + \lambda_{\max}(\boldsymbol{J})\left[(k_{\omega_d} + \lambda_{\max}(\boldsymbol{C}_1))(\delta_\omega k_\omega + \omega_{\min} + \delta_\omega\|\boldsymbol{z}\|)\right. \\
&\quad \left. + (\delta_\varepsilon k_R k_{\omega_d} + \delta_\varepsilon k_\alpha)(\delta_\omega k_\omega + \omega_{\min} + \delta_\omega\|\boldsymbol{z}\| + k_\omega + \|\boldsymbol{z}\|)\right] \\
&\triangleq \boldsymbol{S}(\boldsymbol{z}_2)(\boldsymbol{J}\boldsymbol{\omega}) + \delta_\varepsilon k_{T_1} + \delta_\omega k_\omega k_{T_2} + \omega_{\min} k_{T_2} + \left(\delta_\varepsilon k_{T_3} + \delta_\omega k_{T_2}\right)\|\boldsymbol{z}\|,
\end{aligned} \tag{75}$$

where

$$k_{T_1} \triangleq \lambda_{\max}(\boldsymbol{J})\left(k_R k_{\omega_d} + k_\alpha\right)\left(k_\omega + \delta_\omega k_\omega + \omega_{\min}\right), \tag{76}$$

$$k_{T_2} \triangleq \lambda_{\max}(\boldsymbol{J})\left(k_{\omega_d} + \lambda_{\max}(\boldsymbol{C}_1)\right), \tag{77}$$

$$k_{T_3} \triangleq \lambda_{\max}(\boldsymbol{J})\left(k_R k_{\omega_d} + k_\alpha\right)\left(1 + \delta_\omega\right), \tag{78}$$

and

$$\begin{aligned}
&\|\boldsymbol{S}(\boldsymbol{\omega})\boldsymbol{R}_i^b - \boldsymbol{S}(\boldsymbol{\omega}^{\mathrm{Q}})\boldsymbol{R}_i^{\mathrm{Q}}\| \\
&\leq \|\boldsymbol{\omega}\|\delta_\varepsilon k_R + \|\boldsymbol{d}_\omega\| \\
&\leq \delta_\varepsilon k_\omega k_R + \delta_\omega k_\omega + \omega_{\min} + \left(\delta_\varepsilon k_R + \delta_\omega\right)\|\boldsymbol{z}\|.
\end{aligned} \tag{79}$$

We now state our main result in the following theorem.

Theorem 1. *Consider the closed-loop adaptive system consisting of the plant (26)–(27), the quantized inputs and states (9)–(10) satisfying (11)–(13), the adaptive controller (37)–(38), the parameter update law (39) and Assumptions 1–4. If the gain matrices $\boldsymbol{C}_1$ and $\boldsymbol{C}_2$ and quantization parameters are chosen to satisfy*

$$\frac{c_0}{2} - \delta_{V_2} \geq k > 0, \tag{80}$$

where $c_0 = \min\{\frac{1}{2}\lambda_{\min}(\boldsymbol{C}_1), \lambda_{\min}(\boldsymbol{C}_2)\}$, k is a positive constant, and

$$\delta_{V_2} = \delta_\varepsilon k_{V_1} + \delta_\omega k_{V_2} + \delta_u\left(\delta_\varepsilon k_{u_5} + \delta_\omega k_{u_6} + k_{u_7}\right) + \lambda_{\max}(\boldsymbol{J})\lambda_{\max}(\boldsymbol{C}_1), \tag{81}$$

where

$$k_{V_1} \triangleq k_{T_3} + \lambda_{\max}(\boldsymbol{J})k_R k_{\omega_d}, \tag{82}$$

$$k_{V_2} \triangleq \lambda_{\max}(\boldsymbol{C}_2) + k_{T_2} + \lambda_{\max}(\boldsymbol{J})\left(k_{\omega_d} + 1\right) + k_{\Phi_4}, \tag{83}$$

then, all signals in the closed-loop system are ensured to be uniformly bounded. The $\mathcal{L}_2$-norm of the error states is ultimately bounded by

$$\|\boldsymbol{z}(t)\| \leq \sqrt{\frac{\delta_Q}{k}}, \tag{84}$$

where

$$\delta_Q = \frac{1}{2c_0}\delta_{V_1}^2 + \delta_{V_0}, \tag{85}$$

$$\delta_{V_0} = \delta_\varepsilon k_{\Phi_1} + \delta_\omega k_\omega k_{\Phi_2} + \omega_{\min} k_{\Phi_2}, \tag{86}$$

$$\begin{aligned}\delta_{V_1} = {} & \delta_\varepsilon k_{V_3} + \delta_\omega k_{V_4} + \omega_{\min} k_{V_5} + \delta_u\left(\delta_\varepsilon k_{u_1} + \delta_\omega k_{u_2} + \omega_{\min} k_{u_3} + k_{u_4}\right) \\ & + u_{\min} + \lambda_{\max}(\boldsymbol{J})\lambda_{\max}(\boldsymbol{C}_1)^2,\end{aligned} \tag{87}$$

$$k_{V_3} \triangleq \lambda_{\max}(\boldsymbol{C}_2)k_{z_2} + k_\varepsilon + k_{T_1} + \lambda_{\max}(\boldsymbol{J})\left(k_\omega k_R k_{\omega_d} + k_R k_{\dot{\omega}_d} + k_{\tilde{\alpha}_1}\right) + k_{\Phi_3}, \tag{88}$$

$$k_{V_4} \triangleq k_\omega\left(\lambda_{\max}(\boldsymbol{C}_2) + k_{T_2} + \lambda_{\max}(\boldsymbol{J})k_{\omega_d}\right) + \lambda_{\max}(\boldsymbol{J})k_{\tilde{\alpha}_2} + k_{\Phi_5}, \tag{89}$$

$$k_{V_5} \triangleq \lambda_{\max}(\boldsymbol{C}_2) + k_{T_2} + \lambda_{\max}(\boldsymbol{J})k_{\omega_d} + \lambda_{\max}(\boldsymbol{J})k_{\tilde{\alpha}_2} + k_{\Phi_4}. \tag{90}$$

Tracking of a given reference signal is achieved, with a bounded error.

Proof. We choose a Lyapunov function candidate

$$V(\boldsymbol{z}_1, \boldsymbol{z}_2, \tilde{\boldsymbol{\theta}}, t) = \boldsymbol{z}_1^\top \boldsymbol{z}_1 + \frac{1}{2}\boldsymbol{z}_2^\top \boldsymbol{J}\boldsymbol{z}_2 + \frac{1}{2}\tilde{\boldsymbol{\theta}}^\top \boldsymbol{\Gamma}^{-1}\tilde{\boldsymbol{\theta}}. \tag{91}$$

By following the control design in (37)–(39), the derivative of (91) is given as

$$\begin{aligned}\dot{V} = {} & -\boldsymbol{z}_1^\top \boldsymbol{G}^\top \boldsymbol{C}_1 \boldsymbol{G}\boldsymbol{z}_1 + \boldsymbol{z}_1^\top \boldsymbol{G}^\top \boldsymbol{z}_2 + \boldsymbol{z}_2^\top\big[-\boldsymbol{S}(\boldsymbol{\omega})(\boldsymbol{J}\boldsymbol{\omega}) + \boldsymbol{\Phi}^\top\boldsymbol{\theta} + \boldsymbol{u}^Q \\ & + \boldsymbol{J}\left(\boldsymbol{S}(\boldsymbol{\omega})\boldsymbol{R}_i^b\boldsymbol{\omega}_d - \boldsymbol{R}_i^b\dot{\boldsymbol{\omega}}_d - \dot{\boldsymbol{\alpha}}\right)\big] - \tilde{\boldsymbol{\theta}}^\top\boldsymbol{\Gamma}^{-1}\dot{\hat{\boldsymbol{\theta}}} \\ \leq {} & -\boldsymbol{z}_1^\top \boldsymbol{G}^\top \boldsymbol{C}_1 \boldsymbol{G}\boldsymbol{z}_1 - \boldsymbol{z}_2^\top \boldsymbol{C}_2 \boldsymbol{z}_2^Q + \boldsymbol{z}_2^\top\left(\boldsymbol{G}\boldsymbol{z}_1 - \boldsymbol{G}^Q\boldsymbol{z}_1^Q\right) \\ & + \boldsymbol{z}_2^\top\left[-\boldsymbol{S}(\boldsymbol{\omega})(\boldsymbol{J}\boldsymbol{\omega}) + \boldsymbol{S}(\boldsymbol{R}_i^Q\boldsymbol{\omega}_d)(\boldsymbol{J}\boldsymbol{\omega}^Q) + \boldsymbol{S}(\alpha^Q)(\boldsymbol{J}\boldsymbol{\omega}^Q)\right] \\ & + \boldsymbol{z}_2^\top\boldsymbol{J}\left[\boldsymbol{S}(\boldsymbol{\omega})\boldsymbol{R}_i^b - \boldsymbol{S}(\boldsymbol{\omega}^Q)\boldsymbol{R}_i^Q\right]\boldsymbol{\omega}_d \\ & + \boldsymbol{z}_2^\top\boldsymbol{J}\left(\boldsymbol{R}_i^Q - \boldsymbol{R}_i^b\right)\dot{\boldsymbol{\omega}}_d + \boldsymbol{z}_2^\top\boldsymbol{J}(\tilde{\boldsymbol{\alpha}}^Q - \dot{\boldsymbol{\alpha}}) \\ & + \boldsymbol{z}_2^\top\boldsymbol{d}_u + \left[\boldsymbol{z}_2^\top(\boldsymbol{\Phi}^\top\boldsymbol{\theta} - (\boldsymbol{\Phi}^Q)^\top\hat{\boldsymbol{\theta}}) - \tilde{\boldsymbol{\theta}}^\top\boldsymbol{\Phi}^Q\boldsymbol{z}_2^Q\right].\end{aligned} \tag{92}$$

The last terms in (92) satisfy

$$\begin{aligned}& \boldsymbol{z}_2^\top(\boldsymbol{\Phi}^\top\boldsymbol{\theta} - (\boldsymbol{\Phi}^Q)^\top\hat{\boldsymbol{\theta}}) - \tilde{\boldsymbol{\theta}}^\top\boldsymbol{\Phi}^Q\boldsymbol{z}_2^Q \\ = {} & \boldsymbol{\theta}^\top\boldsymbol{\Phi}\boldsymbol{z}_2 - \boldsymbol{\theta}^\top\boldsymbol{\Phi}^Q\boldsymbol{z}_2 + \tilde{\boldsymbol{\theta}}^\top\boldsymbol{\Phi}^Q\boldsymbol{z}_2 - \tilde{\boldsymbol{\theta}}^\top\boldsymbol{\Phi}^Q\boldsymbol{z}_2^Q \\ \leq {} & \|\boldsymbol{\theta}\|\,\|\boldsymbol{\Phi} - \boldsymbol{\Phi}^Q\|\,\|\boldsymbol{z}_2\| + \|\tilde{\boldsymbol{\theta}}\|\,\|\boldsymbol{\Phi}^Q\|\,\|\boldsymbol{z}_2 - \boldsymbol{z}_2^Q\| \\ \leq {} & k_\theta\|\boldsymbol{\Phi} - \boldsymbol{\Phi}^Q\|\,\|\boldsymbol{z}\| + k_\theta(1 + \|\boldsymbol{\omega}\| + \|\boldsymbol{\Phi} - \boldsymbol{\Phi}^Q\|)\|\boldsymbol{z}_2 - \boldsymbol{z}_2^Q\| \\ \leq {} & \delta_\varepsilon k_{\Phi_1} + \delta_\omega k_\omega k_{\Phi_2} + \omega_{\min}k_{\Phi_2} \\ & + \left(\delta_\varepsilon k_{\Phi_3} + \delta_\omega k_{\Phi_5} + \omega_{\min}k_{\Phi_4}\right)\|\boldsymbol{z}\| + \delta_\omega k_{\Phi_4}\|\boldsymbol{z}\|^2,\end{aligned} \tag{93}$$

where the properties from Lemmas 1–2 are used, and where

$$k_{\Phi_1} \triangleq k_\theta L_1\left(\delta_\varepsilon k_{z_2} + \delta_\omega k_\omega + \omega_{\min}\right) + \left(k_\theta + k_\theta k_\omega\right)k_{z_2}, \tag{94}$$

$$k_{\Phi_2} \triangleq k_\theta L_2\left(\delta_\varepsilon k_{z_2} + \delta_\omega k_\omega + \omega_{\min}\right) + \left(k_\theta + k_\theta k_\omega\right), \tag{95}$$

$$k_{\Phi_3} \triangleq k_\theta L_1\left(1 + \delta_\omega\right) + k_\theta k_{z_2}, \tag{96}$$

$$k_{\Phi_4} \triangleq k_\theta\left(1 + L_2 + L_2\delta_\omega\right), \tag{97}$$

$$k_{\Phi_5} \triangleq k_{\Phi_2} + k_\omega k_{\Phi_4}. \tag{98}$$

By using the properties from Lemmas 1–4 together with (75), (79) and (93) and using Young's inequality, we have

$$\begin{aligned}\dot{V} \leq {} & -c_0\|\boldsymbol{z}\|^2 + \delta_{V_0} + \delta_{V_1}\|\boldsymbol{z}\| + \delta_{V_2}\|\boldsymbol{z}\|^2 \\ \leq {} & -\left(\frac{c_0}{2} - \delta_{V_2}\right)\|\boldsymbol{z}\|^2 + \frac{1}{2c_0}\delta_{V_1}^2 + \delta_{V_0} \\ \leq {} & -k\|\boldsymbol{z}\|^2 + \delta_Q < 0, \quad \forall\|\boldsymbol{z}\| > \sqrt{\delta_Q/k}.\end{aligned} \tag{99}$$

This shows that the ultimate bound for $\boldsymbol{z}(t)$ satisfies (84) under condition (80). Since $\boldsymbol{z}$ is bounded, then by Lemma 2, $\boldsymbol{z}^Q$ is bounded. Then the estimated parameter vector $\hat{\boldsymbol{\theta}}$ is ensured bounded by the projection operator (39). Since $\boldsymbol{z}$ is bounded, then by Lemmas 1–3 and the property of unity of the unit quaternion, all signals in the closed loop are ensured bounded. □

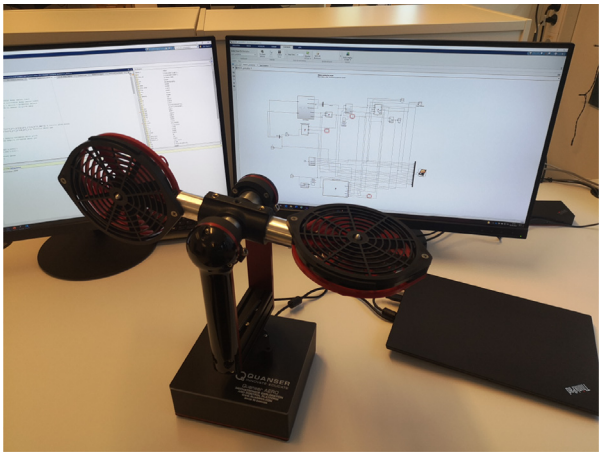

Fig. 5. Quanser Aero helicopter system connected with computer.

Remark 5. The quantization parameters should be chosen to guarantee the stability and control performances of the attitude tracking control system, and (80) give some insight to this. Since both the control signals and the states are shown to be bounded, the required number of quantization levels are finite and only a finite number of quantization levels are required to stabilize the system. It can be observed from (85)–(87) that the upper bound of the errors in the sense of (84) can be decreased if the quantization parameters $\delta_{(\cdot)}$, $\omega_{\min}$ and $u_{\min}$ are decreased, while all design parameters $\boldsymbol{C}_{(\cdot)}$ are kept unchanged. The choice of quantization parameters will depend on the application and the available data-rate for the communication network.

Remark 6. A logarithmic quantizer has a better resolution close to zero. Since we are considering a tracking problem where the states are quantized and not the error states, this would also imply that the error from quantization will be larger if the reference signal is far from the origin. For tracking of a reference signal further away from the equilibrium, one option is to use a logarithmic-uniform quantizer, described in Section 2.4.3, for the state signals. For the stability analysis, this only imply that $\delta_\omega = 0$, and the value of δ_ε is smaller, which again implies that the error signals will converge towards a smaller compact set.

Remark 7. Time-delays in the communication channels have significant effects in networked control systems, where the presence of delays may result in a poor performance and can also lead to instability, see e.g. [4,34]. Extending present results to handle both quantization and time-delay is nontrivial, and is an interesting problem to investigate further.

Table 1
Helicopter parameters.

Symbol	Value	Units
$\boldsymbol{J}$	diag(0.0218, 0.0217, 0.0218)	kgm^2
m	1.075	kg
g	9.81	m/s^2
$\boldsymbol{R}_b^g$	$[0 \quad 0 \quad -0.0038]^\top$	m

5. Experimental results

To illustrate the presented adaptive control scheme, we implemented the controller on the Quanser Aero helicopter system, shown in Fig. 5. This is a two-rotor laboratory equipment for flight control-based experiments. With a horizontal position of the main thruster and a vertical position of the tail thruster, this resembles a helicopter with two propellers driven by two DC motors. The helicopter is a MIMO system with 2 DOF, and can rotate around two axes where each input affects both rotational directions. The dynamic equation for the helicopter model is defined as

$$\boldsymbol{J}\dot{\boldsymbol{\omega}} = -\boldsymbol{S}(\boldsymbol{\omega})(\boldsymbol{J}\boldsymbol{\omega}) + \Phi(\boldsymbol{\varepsilon}, \boldsymbol{\omega})^\top \boldsymbol{\theta} + \boldsymbol{u}^{\mathrm{Q}} - \boldsymbol{g}(\boldsymbol{q}) + \boldsymbol{\tau}_g, \tag{100}$$

where $\boldsymbol{g}(\boldsymbol{q}) = -\boldsymbol{S}(\boldsymbol{r}_g^b)\boldsymbol{R}_i^b \boldsymbol{f}_g^i \in \mathbb{R}^3$, $\boldsymbol{r}_g^b = [x_g \; y_g \; z_g]^\top$ is the distance from the origin to the center of mass, $\boldsymbol{f}_g^i = [0 \;\; 0 \;\; -mg]^\top$, m is the mass of the rigid body, and g is the gravitational acceleration. The torque $\boldsymbol{g}(\boldsymbol{q})$ is caused by the gravitational force, because the rotation of the helicopter is not about the center of mass. We assume that this torque can be compensated for directly by measurements of $\boldsymbol{q}$, where $\boldsymbol{\tau}_g = \boldsymbol{g}(\boldsymbol{q})$, and is not sent over the network. The mathematical model is then described by (1)–(2), and the system receives the driving toques $\boldsymbol{\tau} = \boldsymbol{u}^{\mathrm{Q}} + \boldsymbol{\tau}_g$. The parameters used for simulation and experiments are shown in Table 1, where $\Phi = \mathrm{diag}(-\boldsymbol{\omega})$, the initial states and estimated parameters were chosen as $\boldsymbol{q}(t_0) = [1\ 0\ 0\ 0]^\top$, $\boldsymbol{\omega}(t_0) = [0\ 0\ 0]^\top$ and $\hat{\boldsymbol{\theta}}(t_0) = [0\ 0.0070\ 0.0095]^\top$, where t_0 defines the start of experiment, and the design parameters were set to $\boldsymbol{C}_1 = 0.3\boldsymbol{I}$, $\boldsymbol{C}_2 = 0.15\boldsymbol{I}$ and $\boldsymbol{\Gamma} = 0.02\boldsymbol{I}$. The quantization parameters were chosen as $\delta_{\varepsilon_i} = \delta_{\omega_i} = 0.02$, $\varepsilon_{0_i} = \omega_{0_i} = 0.005$ $i = 1, 2, 3$ for the states, and $\delta_{u_i} = 0.05$, $u_{0_i} = 0.0055$ $i = 1, 2, 3$ for the inputs. For the chosen values, Eq. (80) holds. The term $\Phi(\boldsymbol{\omega})^\top\boldsymbol{\theta}$ in the dynamical model of the practical setup relates to viscous damping in the system. The true values of the damping coefficients $\boldsymbol{\theta}$ are not known, and the update law (39) for the estimated values does not provide convergence towards the true values. The objective in the experiment was to track a given sinusoidal signal for the attitude, where $r_d = 0$, $p_d = 20\pi/180\sin(0.1\pi t + \pi/2)$, $y_d = 20\pi/180\sin(0.05\pi t + \pi/2)$, given in Euler angles, that was converted to a quaternion, and also to track the angular velocities as given in (17), while the inputs sent to the helicopter and the measured states sent to the controller were quantized. The initial value for the desired attitude was $\boldsymbol{q}_d(t_0) = [0.9698, \; -0.0302, \; 0.1710, \; 0.1710]^\top$ and so initially we have a tracking error $\boldsymbol{e}^{\mathrm{Q}}(t_0) = [0.9698, 0.0302, -0.1710, -0, 1710]^\top$, see Eq. (35). Since $\mathrm{sgn}(\tilde{\eta}^{\mathrm{Q}}(t_0)) \geq 0$, we choose the positive equilibrium point (40) for our maneuver.

Figs. 6–10 show the attitude $\boldsymbol{\varepsilon}^{\mathrm{Q}}$, the angular velocity $\boldsymbol{\omega}^{\mathrm{Q}}$, the error in attitude $\tilde{\boldsymbol{\varepsilon}}^{\mathrm{Q}}$, the error in angular velocity $\boldsymbol{\omega}_e^{\mathrm{Q}}$, and the inputs $\boldsymbol{u}^{\mathrm{Q}}$, respectively. The dotted lines show the desired reference signals, while measured values from experiments on the helicopter system are shown with a solid line. The same experiment was also conducted with continuous measurements of the inputs and the states with results given in Figs. 11–13

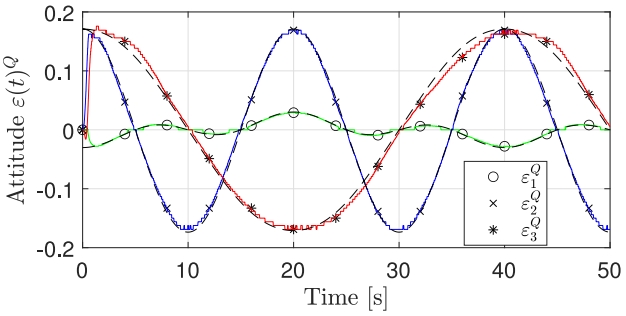

Fig. 6. Attitude $\boldsymbol{\varepsilon}^{\mathrm{Q}}$ from experiment with quantization.

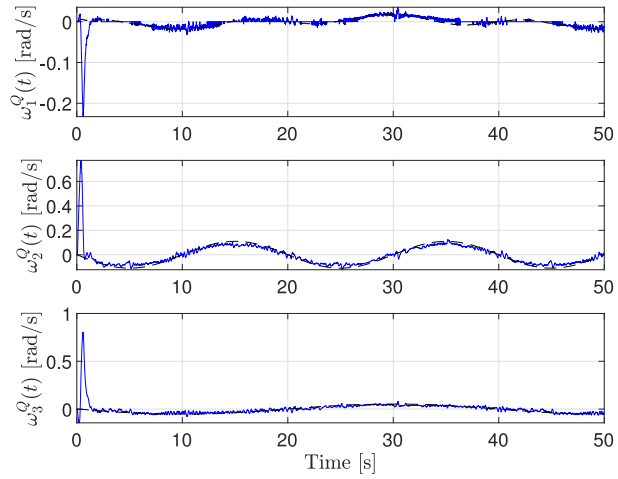

Fig. 7. Angular velocity $\boldsymbol{\omega}^{\mathrm{Q}}$ from experiment with quantization.

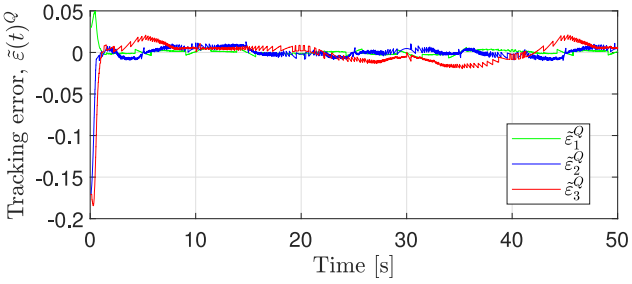

Fig. 8. Tracking error $\tilde{\boldsymbol{\varepsilon}}^{\mathrm{Q}}$ from experiment with quantization.

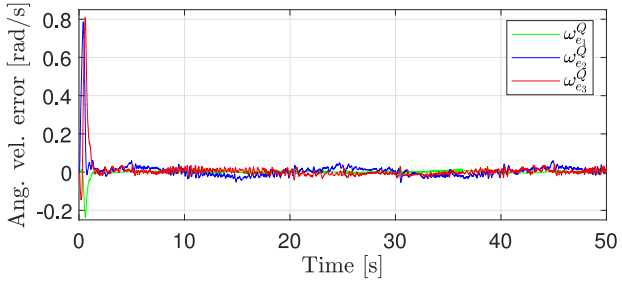

Fig. 9. Angular velocity error $\boldsymbol{\omega}_e^{\mathrm{Q}}$ from experiment with quantization.

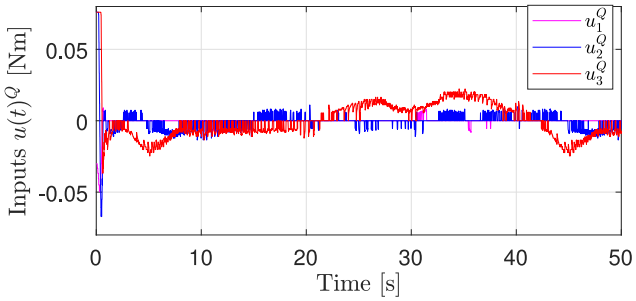

Fig. 10. Inputs $\boldsymbol{u}^Q$ from experiment with quantization.

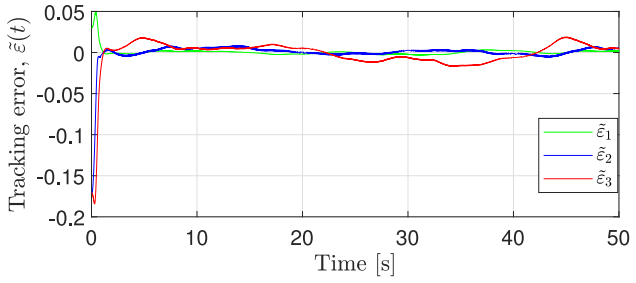

Fig. 11. Tracking error $\tilde{\boldsymbol{\varepsilon}}$ from experiment without quantization.

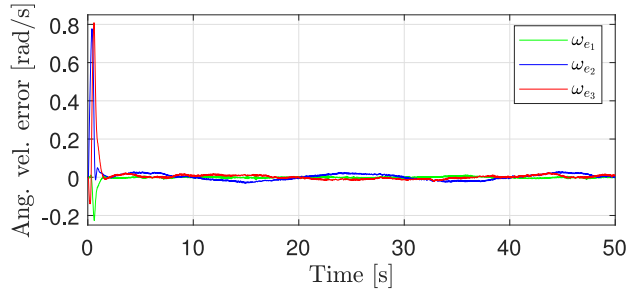

Fig. 12. Angular velocity error $\boldsymbol{\omega}_e$ from experiment without quantization.

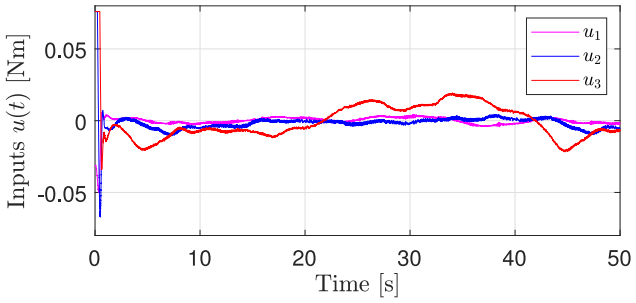

Fig. 13. Inputs $\boldsymbol{u}$ from experiment without quantization.

showing the error in attitude $\tilde{\boldsymbol{\varepsilon}}$, the error in angular velocity $\boldsymbol{\omega}_e$, and the inputs $\boldsymbol{u}$, respectively.

For both cases, the inputs and the states are shown to be bounded, and tracking is achieved with a bounded tracking error. The total tracking error was defined as

$$z_{\text{track}} = \int_{t_0}^{t_f} (\tilde{\boldsymbol{\varepsilon}}^Q)^\top \tilde{\boldsymbol{\varepsilon}}^Q d\tau, \tag{101}$$

Table 2
Tracking error with and without quantization.

$z_{\text{track}} \times 10^{-4}$		State	
		Continuous	Quantized
Input	Continuous	311	315
	Quantized	318	320

where t_0 and t_f define start and end of experiment, respectively. The experiments were run for 50 s and results are provided in Table 2, and is an average of three runs for each case. The tracking error is increased by introducing quantization as expected. As the results show, a good performance can be maintained by introducing quantization, while at the same time the communication burden over a network can be decreased.

6. Conclusion

An adaptive backstepping control design has been developed for attitude tracking of rigid body systems with uncertain parameters and with quantization of both inputs and states. Since there exist two equilibria using unit quaternions, a target equilibrium point is chosen before starting the maneuver, and thus one is regulated to the closest equilibrium point. This will avoid the problem of unwinding. A class of sector bounded quantizers has been considered, which introduce quantization errors that are linearly dependent on the inputs to the quantizers. All signals in the closed loop system are shown to be uniformly bounded and tracking of a given reference signal is achieved. The tracking performance is also established and can be improved by appropriately adjusting design parameters. The choice of quantization parameters directly affects the size of the equilibrium set, and this relationship is shown in the analysis. Experiments on a 2-DOF helicopter system illustrate the proposed control scheme.

CRediT authorship contribution statement

Siri Marte Schlanbusch: Methodology, Simulation, Experiment, Writing – original draft. **Jing Zhou:** Resources, Validation, Supervision, Writing – review & editing, Funding acquisition.

Declaration of competing interest

The authors declare that they have no known competing financial interests or personal relationships that could have appeared to influence the work reported in this paper.

Data availability

No data was used for the research described in the article.

Appendix A. Proof of Lemma 1

From (24) we have

$$\|\boldsymbol{\alpha}\| \leq \lambda_{\max}(\boldsymbol{C}_1)\|\tilde{\boldsymbol{\varepsilon}}\| \leq \lambda_{\max}(\boldsymbol{C}_1), \tag{A.1}$$

where $\|\tilde{\boldsymbol{\varepsilon}}\| \leq 1$. From (20), (23) and Assumption 1, the angular velocity error and angular velocity satisfy

$$\|\boldsymbol{\omega}_e\| \leq \|\boldsymbol{z}_2 + \boldsymbol{\alpha}\| \leq \lambda_{\max}(\boldsymbol{C}_1) + \|\boldsymbol{z}\|, \tag{A.2}$$

$$\|\boldsymbol{\omega}\| \leq \|\boldsymbol{\omega}_e + \boldsymbol{R}_i^b \boldsymbol{\omega}_d\| \leq \lambda_{\max}(\boldsymbol{C}_1) + k_{\omega_d} + \|\boldsymbol{z}\| \triangleq k_\omega + \|\boldsymbol{z}\|, \tag{A.3}$$

where $\boldsymbol{z} = [\boldsymbol{z}_1^\top, \boldsymbol{z}_2^\top]^\top$. □

Appendix B. Proof of Lemma 2

By using (34) and (47) and the property of (5) and (6), we have

$$\begin{aligned}\|\boldsymbol{R}_i^Q - \boldsymbol{R}_i^b\| &= \|\boldsymbol{R}_b^Q\boldsymbol{R}_i^b - \boldsymbol{R}_i^b\| = \|(\boldsymbol{R}_b^Q - \boldsymbol{I})\boldsymbol{R}_i^b\| \\ &\le \|-2d_\eta \boldsymbol{S}(\boldsymbol{d}_{\tilde{\varepsilon}}) + 2\boldsymbol{S}^2(\boldsymbol{d}_{\tilde{\varepsilon}})^\top\| \, \|\boldsymbol{R}_i^b\| \\ &\le \delta_\varepsilon \left(2k_\varepsilon + 2k_\varepsilon^2\delta_\varepsilon\right) \triangleq \delta_\varepsilon k_R. \end{aligned} \tag{B.1}$$

From the definition in (36) and the fact that $\boldsymbol{G}\boldsymbol{z}_1 = \pm\tilde{\boldsymbol{\varepsilon}}$ and $\boldsymbol{G}^Q\boldsymbol{z}_1^Q = \pm\tilde{\boldsymbol{\varepsilon}}^Q$, it is shown that

$$\|\boldsymbol{G}^Q\boldsymbol{z}_1^Q - \boldsymbol{G}\boldsymbol{z}_1\| = \|(\pm\tilde{\boldsymbol{\varepsilon}}^Q) - (\pm\tilde{\boldsymbol{\varepsilon}})\| \le \|\boldsymbol{d}_{\tilde{\varepsilon}}\| \le \delta_\varepsilon k_\varepsilon. \tag{B.2}$$

From (24), (43) and (53) we have

$$\|\boldsymbol{\alpha}^Q - \boldsymbol{\alpha}\| = \|(-\boldsymbol{C}_1\boldsymbol{G}^Q\boldsymbol{z}_1^Q) - (-\boldsymbol{C}_1\boldsymbol{G}\boldsymbol{z}_1)\| \le \lambda_{\max}(\boldsymbol{C}_1)k_\varepsilon\delta_\varepsilon \triangleq \delta_\varepsilon k_\alpha. \tag{B.3}$$

From (12) and (50) we have

$$\|\boldsymbol{\omega}^Q - \boldsymbol{\omega}\| \le \delta_\omega\|\boldsymbol{\omega}\| + \omega_{\min} \le \delta_\omega k_\omega + \omega_{\min} + \delta_\omega\|\boldsymbol{z}\|. \tag{B.4}$$

With the use of (46), (47) and (55) we have

$$\begin{aligned}\|\boldsymbol{\omega}_e^Q - \boldsymbol{\omega}_e\| &= \|\boldsymbol{\omega}^Q - \boldsymbol{R}_i^Q\boldsymbol{\omega}_d - (\boldsymbol{\omega} - \boldsymbol{R}_i^b\boldsymbol{\omega}_d)\| \\ &\le \delta_\varepsilon k_R k_{\omega_d} + \delta_\omega k_\omega + \omega_{\min} + \delta_\omega\|\boldsymbol{z}\|. \end{aligned} \tag{B.5}$$

Using (23), (41), (54) and (56), we have

$$\begin{aligned}\|\boldsymbol{z}_2^Q - \boldsymbol{z}_2\| &\le \|\boldsymbol{\omega}_e^Q - \boldsymbol{\alpha}^Q - (\boldsymbol{\omega}_e - \boldsymbol{\alpha})\| \\ &\le \delta_\varepsilon(k_R k_{\omega_d} + k_\alpha) + \delta_\omega k_\omega + \omega_{\min} + \delta_\omega\|\boldsymbol{z}\| \\ &\triangleq \delta_\varepsilon k_{z_2} + \delta_\omega k_\omega + \omega_{\min} + \delta_\omega\|\boldsymbol{z}\|. \end{aligned} \tag{B.6}$$

By using (28), (45), (49) and (56), we have

$$\begin{aligned}\|\bar{\boldsymbol{\alpha}}^Q - \dot{\boldsymbol{\alpha}}\| &= \|\frac{1}{2}\boldsymbol{C}_1\left[\mp[\tilde{\eta}^Q\boldsymbol{I} + \boldsymbol{S}(\tilde{\boldsymbol{\varepsilon}}^Q)]\boldsymbol{\omega}_e^Q - [\mp[\tilde{\eta}\boldsymbol{I} + \boldsymbol{S}(\tilde{\boldsymbol{\varepsilon}})]]\boldsymbol{\omega}_e\right]\| \\ &\le \frac{1}{2}\lambda_{\max}(\boldsymbol{C}_1)\left(2\|\boldsymbol{\omega}_e\| + \delta_\varepsilon k_R k_{\omega_d} + \delta_\omega k_\omega + \omega_{\min} + \delta_\omega\|\boldsymbol{z}\|\right) \\ &\triangleq \delta_\varepsilon k_{\bar{\alpha}_1} + \delta_\omega k_{\bar{\alpha}_2} + \omega_{\min}k_{\bar{\alpha}_3} + \lambda_{\max}(\boldsymbol{C}_1)^2 \\ &\quad + (\lambda_{\max}(\boldsymbol{C}_1) + \delta_\omega)\|\boldsymbol{z}\|. \end{aligned} \tag{B.7}$$

From Assumption 3, the unity property of unit quaternion and from (55) we have

$$\begin{aligned}\|\Phi^Q - \Phi\| &\le L_1\|\boldsymbol{\varepsilon}^Q - \boldsymbol{\varepsilon}\| + L_2\|\boldsymbol{\omega}^Q - \boldsymbol{\omega}\| \\ &\le \delta_\varepsilon L_1 + \delta_\omega L_2 k_\omega + \omega_{\min}L_2 + \delta_\omega L_2\|\boldsymbol{z}\|. \quad \square \end{aligned} \tag{B.8}$$

Appendix C. Proof of Lemma 3

The norm of the control input $\boldsymbol{u}$ in (38) satisfies the following inequality

$$\begin{aligned}\|\boldsymbol{u}\| &= \| - \boldsymbol{G}^Q\boldsymbol{z}_1^Q - \boldsymbol{C}_2\boldsymbol{z}_2^Q - (\Phi^Q)^\top\hat{\boldsymbol{\theta}} + \boldsymbol{S}(\boldsymbol{R}_i^Q\boldsymbol{\omega}_d)(\boldsymbol{J}\boldsymbol{\omega}^Q) \\ &\quad + \boldsymbol{S}(\boldsymbol{\alpha}^Q)(\boldsymbol{J}\boldsymbol{\omega}^Q) - \boldsymbol{J}\left(\boldsymbol{S}(\boldsymbol{\omega}^Q)\boldsymbol{R}_i^Q\boldsymbol{\omega}_d - \boldsymbol{R}_i^Q\dot{\boldsymbol{\omega}}_d - \bar{\boldsymbol{\alpha}}^Q\right)\| \\ &\le 1 + \delta_\varepsilon k_\varepsilon + \lambda_{\max}(\boldsymbol{C}_2)\left(\delta_\varepsilon k_{z_2} + \delta_\omega k_\omega + \omega_{\min} + \delta_\omega\|\boldsymbol{z}\| + \|\boldsymbol{z}_2\|\right) \\ &\quad + k_\theta\left(\delta_\varepsilon L_1 + \delta_\omega L_2 k_\omega + \omega_{\min}L_2 + \delta_\omega L_2\|\boldsymbol{z}\| + \|\boldsymbol{\varepsilon}\| + \|\boldsymbol{\omega}\|\right) \\ &\quad + \lambda_{\max}(\boldsymbol{J})\left(2k_{\omega_d} + \|\boldsymbol{\alpha}\| + \delta_\varepsilon k_\alpha\right)\|\boldsymbol{\omega}^Q\| \\ &\quad + \lambda_{\max}(\boldsymbol{J})\left(k_{\dot{\omega}_d} + \|\bar{\boldsymbol{\alpha}}^Q\|\right) \\ &\triangleq \delta_\varepsilon k_{u_1} + \delta_\omega k_{u_2} + \omega_{\min}k_{u_3} + k_{u_4} + \delta_\varepsilon k_{u_5}\|\boldsymbol{z}\| + \delta_\omega k_{u_6}\|\boldsymbol{z}\| + k_{u_7}\|\boldsymbol{z}\|, \end{aligned} \tag{C.1}$$

where we have used the properties from Lemmas 1 and 2. Then

$$\begin{aligned}\|\boldsymbol{u}^Q - \boldsymbol{u}\| &\le \delta_u\|\boldsymbol{u}\| + u_{\min} \\ &\le \delta_u\left(\delta_\varepsilon k_{u_1} + \delta_\omega k_{u_2} + \omega_{\min}k_{u_3} + k_{u_4}\right) + u_{\min} \\ &\quad + \delta_u\left(\delta_\varepsilon k_{u_5} + \delta_\omega k_{u_6} + k_{u_7}\right)\|\boldsymbol{z}\|. \quad \square \end{aligned} \tag{C.2}$$

Appendix D. Proof of Lemma 4

We use the property

$$0 \le (1 \mp \tilde{\eta})^2 \le (1 - \tilde{\eta})(1 + \tilde{\eta}) = \tilde{\boldsymbol{\varepsilon}}^\top\tilde{\boldsymbol{\varepsilon}}, \tag{D.1}$$

that holds by Assumption 4. Then

$$(1 \mp \tilde{\eta})^2 + \tilde{\boldsymbol{\varepsilon}}^\top\tilde{\boldsymbol{\varepsilon}} \le 2\tilde{\boldsymbol{\varepsilon}}^\top\tilde{\boldsymbol{\varepsilon}} \tag{D.2}$$

$$\frac{1}{2}\boldsymbol{z}_1^\top\boldsymbol{z}_1 \le \tilde{\boldsymbol{\varepsilon}}^\top\tilde{\boldsymbol{\varepsilon}} \tag{D.3}$$

$$\frac{1}{2}\lambda_{\min}(\boldsymbol{C}_1)\boldsymbol{z}_1^\top\boldsymbol{z}_1 \le \tilde{\boldsymbol{\varepsilon}}^\top\boldsymbol{C}_1\tilde{\boldsymbol{\varepsilon}} = \boldsymbol{z}_1^\top\boldsymbol{G}^\top\boldsymbol{C}_1\boldsymbol{G}\boldsymbol{z}_1. \quad \square \tag{D.4}$$

References

[1] N. Elia, S.K. Mitter, Stabilization of linear systems with limited information, IEEE Trans. Automat. Control 46 (9) (2001) 1384–1400, http://dx.doi.org/10.1109/9.948466.

[2] R.W. Brockett, D. Liberzon, Quantized feedback stabilization of linear systems, IEEE Trans. Automat. Control 45 (7) (2000) 1279–1289, http://dx.doi.org/10.1109/9.867021.

[3] C.-Y. Kao, S.R. Venkatesh, Stabilization of linear systems with limited information multiple input case, in: Proceedings of the 2002 American Control Conference (IEEE Cat. No. CH37301), IEEE, 2002, http://dx.doi.org/10.1109/acc.2002.1024003.

[4] E. Fridman, M. Dambrine, Control under quantization, saturation and delay: An LMI approach, Automatica 45 (10) (2009) 2258–2264, http://dx.doi.org/10.1016/j.automatica.2009.05.020.

[5] J. Liu, N. Elia, Quantized feedback stabilization of non-linear affine systems, Internat. J. Control 77 (3) (2004) 239–249, http://dx.doi.org/10.1080/00207170310001655336.

[6] T. Hayakawa, H. Ishii, K. Tsumaru, Adaptive quantized control for nonlinear uncertain systems, Systems Control Lett. 58 (9) (2009) 625–632, http://dx.doi.org/10.1016/j.sysconle.2008.12.007.

[7] J. Zhou, C. Wen, Adaptive backstepping control of uncertain nonlinear systems with input quantization, in: IEEE Conference on Decision and Control, 2013, pp. 5571–5576, http://dx.doi.org/10.1109/CDC.2013.6760767.

[8] C.D. Persis, Robust stabilization of nonlinear systems by quantized and ternary control, Systems Control Lett. 58 (8) (2009) 602–608, http://dx.doi.org/10.1016/j.sysconle.2009.04.003.

[9] J. Zhou, C. Wen, G. Yang, Adaptive backstepping stabilization of nonlinear uncertain systems with quantized input signal, IEEE Trans. Autom. Control 59 (2) (2014) 460–464, http://dx.doi.org/10.1109/TAC.2013.2270870.

[10] L. Xing, C. Wen, Y. Zhu, H. Su, Z. Liu, Output feedback control for uncertain nonlinear systems with input quantization, Automatica 65 (2015) 191–202, http://dx.doi.org/10.1016/j.automatica.2015.11.028.

[11] J. Zhou, W. Wang, Adaptive control of quantized uncertain nonlinear systems, IFAC PapersOnLine 50 (1) (2017) 10425–10430, http://dx.doi.org/10.1016/j.ifacol.2017.08.1970.

[12] Y. Li, G. Yang, Adaptive asymptotic tracking control of uncertain nonlinear systems with input quantization and actuator faults, Automatica 72 (2016) 177–185, http://dx.doi.org/10.1016/j.automatica.2016.06.008.

[13] L. Xing, C. Wen, H. Su, Z. Liu, J. Cai, Robust control for a class of uncertain nonlinear systems with input quantization, Internat. J. Robust Nonlinear Control 26 (8) (2015) 1585–1596, http://dx.doi.org/10.1002/rnc.3367.

[14] Y. Wang, L. He, C. Huang, Adaptive time-varying formation tracking control of unmanned aerial vehicles with quantized input, ISA Trans. 85 (2019) 76–83, http://dx.doi.org/10.1016/j.isatra.2018.09.013.

[15] B. Huang, B. Zhou, S. Zhang, C. Zhu, Adaptive prescribed performance tracking control for underactuated autonomous underwater vehicles with input quantization, Ocean Eng. 221 (2021) http://dx.doi.org/10.1016/j.oceaneng.2020.108549.

[16] S.M. Schlanbusch, J. Zhou, Adaptive backstepping control of a 2-DOF helicopter system with uniform quantized inputs, in: IECON 2020 the 46th Annual Conference of the IEEE Industrial Electronics Society, 2020, pp. 88–94, http://dx.doi.org/10.1109/iecon43393.2020.9254497.

[17] A. Selivanov, A. Fradkov, D. Liberzon, Adaptive control of passifiable linear systems with quantized measurements and bounded disturbances, Systems Control Lett. 88 (2016) 62–67, http://dx.doi.org/10.1016/j.sysconle.2015.12.001.

[18] A. Margun, I. Furtat, A. Kremlev, Robust control of twin rotor MIMO system with quantized output, IFAC-PapersOnLine 50 (1) (2017) 4849–4854, http://dx.doi.org/10.1016/j.ifacol.2017.08.973.

[19] J. Zhou, C. Wen, W. Wang, F. Yang, Adaptive backstepping control of nonlinear uncertain systems with quantized states, IEEE Trans. Automat. Control 64 (11) (2019) 4756–4763, http://dx.doi.org/10.1109/TAC.2019.2906931.

[20] S.M. Schlanbusch, J. Zhou, R. Schlanbusch, Adaptive backstepping attitude control of a rigid body with state quantization, in: Proceedings of 60th IEEE Conference on Decision and Control, 2021, pp. 372–377, http://dx.doi.org/10.1109/CDC45484.2021.9683579.
[21] D.F. Coutinho, M. Fu, C.E. de Souza, Input and output quantized feedback linear systems, IEEE Trans. Automat. Control 55 (3) (2010) 761–766, http://dx.doi.org/10.1109/tac.2010.2040497.
[22] Y. Yan, S. Yu, Sliding mode tracking control of autonomous underwater vehicles with the effect of quantization, Ocean Eng. 151 (2018) 322–328, http://dx.doi.org/10.1016/j.oceaneng.2018.01.034.
[23] Y. Yan, S. Yu, C. Sun, Quantization-based event-triggered sliding mode tracking control of mechanical systems, Inform. Sci. 523 (2020) 296–306, http://dx.doi.org/10.1016/j.ins.2020.03.023.
[24] S.J. Yoo, B.S. Park, Quantized-states-based adaptive control against unknown slippage effects of uncertain mobile robots with input and state quantization, Nonlinear Anal. Hybrid Syst. 42 (2021) 1–17, http://dx.doi.org/10.1016/j.nahs.2021.101077, article 101077.
[25] B.M. Kim, S.J. Yoo, Approximation-based quantized state feedback tracking of uncertain input-saturated MIMO nonlinear systems with application to 2-DOF helicopter, Mathematics 9 (9) (2021) http://dx.doi.org/10.3390/math9091062.
[26] S.M. Schlanbusch, J. Zhou, R. Schlanbusch, Adaptive attitude control of a rigid body with input and output quantization, IEEE Trans. Ind. Electron. 69 (8) (2022) 8296–8305, http://dx.doi.org/10.1109/tie.2021.3105999.
[27] W. Wang, J. Zhou, C. Wen, J. Long, Adaptive backstepping control of uncertain nonlinear systems with input and state quantization, IEEE Trans. Automat. Control (2021) http://dx.doi.org/10.1109/tac.2021.3131958.
[28] J.C.K. Chou, Quaternion kinematic and dynamic differential equations, IEEE Trans. Robot. Autom. 8 (1) (1992) 53–64, http://dx.doi.org/10.1109/70.127239.
[29] T.I. Fossen, Marine Control Systems: Guidance, Navigation, and Control of Ships, Rigs and Underwater Vehicles, Marine Cybernetics AS, Trondheim, Norway, 2002.
[30] O. Egeland, J.T. Gravdahl, Modeling and Simulation for Automatic Control, Marine Cybernetics AS, 2003.
[31] C.G. Mayhew, R.G. Sanfelice, A.R. Teel, Quaternion-based hybrid control for robust global attitude tracking, IEEE Trans. Automat. Control 56 (11) (2011) 2555–2566, http://dx.doi.org/10.1109/tac.2011.2108490.
[32] J. Zhou, L. Xing, C. Wen, Adaptive Control of Dynamic Systems with Uncertainty and Quantization, CRC Press, 2021, http://dx.doi.org/10.1201/9781003176626.
[33] J. Zhou, C. Wen, W. Wang, Adaptive control of uncertain nonlinear systems with quantized input signal, Automatica 95 (2018) 152–162, http://dx.doi.org/10.1016/j.automatica.2018.05.014.
[34] C.D. Persis, F. Mazenc, Stability of quantized time-delay nonlinear systems: a Lyapunov–Krasowskii-functional approach, Math. Control Signals Systems 21 (4) (2010) 337–370, http://dx.doi.org/10.1007/s00498-010-0048-1.
[35] M. Malcangi, Introduction - digital audio, 1995, Online, URL https://www.lim.di.unimi.it/IEEE/MALCANGI/B/INTRO.HTM. (Accessed January 2023).
[36] Q. Shen, C. Yue, C.H. Goh, B. Wu, D. Wang, Rigid-body attitude tracking control under actuator faults and angular velocity constraints, IEEE/ASME Trans. Mechatronics 23 (3) (2018) 1338–1349, http://dx.doi.org/10.1109/tmech.2018.2812871.
[37] L.-J. Liu, J. Zhou, C. Wen, X. Zhao, Robust adaptive tracking control of uncertain systems with time-varying input delays, Internat. J. Systems Sci. 48 (16) (2017) 3440–3449, http://dx.doi.org/10.1080/00207721.2017.1382604.
[38] A. Benallegue, Y. Chitour, A. Tayebi, Adaptive attitude tracking control of rigid body systems with unknown inertia and gyro-bias, IEEE Trans. Automat. Control 63 (11) (2018) 3986–3993, http://dx.doi.org/10.1109/tac.2018.2808443.
[39] M. Krstić, I. Kanellakopoulos, P. Kokotović, Nonlinear and Adaptive Control Design, John Wiley & Sons, Inc., 1995.
[40] R. Schlanbusch, A. Loria, P.J. Nicklasson, On the stability and stabilization of quaternion equilibria of rigid bodies, Automatica 48 (12) (2012) 3135–3141, http://dx.doi.org/10.1016/j.automatica.2012.08.012.